THE ASTRONOMICAL JOURNAL, 115:1869–1887, 1998 May

A WIDE FIELD PLANETARY CAMERA 2 STUDY OF THE RESOLVED STELLAR POPULATION OF THE PEGASUS DWARF IRREGULAR GALAXY (DDO 216)[1]

J. S. GALLAGHER
Department of Astronomy, University of Wisconsin, 475 North Charter Street, Madison, WI 53706-1582; jsg@tiger.astro.wisc.edu
E. TOLSTOY
Space Telescope European Coordinating Facility, ESO, Karl-Schwarzschild-Strasse 2, D-85748 Garching bei München, Germany
ROBBIE C. DOHM-PALMER AND E. D. SKILLMAN
Department of Astronomy, University of Minnesota, 116 Church Street, SE, Minneapolis, MN 55455
A. A. COLE AND J. G. HOESSEL
Department of Astronomy, University of Wisconsin, 475 North Charter Street, Madison, WI 53706-1582
A. SAHA
Space Telescope Science Institute, 3700 San Martin Drive, Baltimore, MD 21218
AND
M. MATEO
Department of Astronomy, University of Michigan, 821 Dennison Building, Ann Arbor, MI 48109-1090
Received 1997 October 27; revised 1998 January 15

ABSTRACT

The stellar population of the Pegasus dwarf irregular galaxy is investigated in images taken in the F439W (*B*), F555W (*V*), and F814W (*I*) bands with the Wide Field Planetary Camera 2 (WFPC2) on the *Hubble Space Telescope*. With WFPC2 the Pegasus dwarf is highly resolved into individual stars to limiting magnitudes of about 25.5 in *B* and *V* and 25 in *I*. These and ground-based data are combined to produce color-magnitude diagrams that show the complex nature of the stellar population in this small galaxy. A young (<0.5 Gyr) main-sequence stellar component is present and clustered in two centrally located clumps, while older stars form a more extended disk or halo. The colors of the main sequence require a relatively large extinction of $A_V = 0.47$ mag. The mean color of the well-populated red giant branch (RGB) is relatively blue, consistent with a moderate-metallicity young, or older metal-poor, stellar population. The RGB also has significant width in color, implying a range of stellar ages and/or metallicities. A small number of extended asymptotic giant branch stars are found beyond the RGB tip. Near the faint limits of our data is a populous red clump superposed on the RGB. Efforts to fit self-consistent stellar population models based on the Geneva stellar evolutionary tracks yield a revised distance of 760 kpc. Quantitative fits to the stellar population are explored as a means of constraining the star formation history. The numbers of main-sequence and core helium burning blue-loop stars require that the star formation rate was higher in the recent past, by a factor of 3–4 about 1 Gyr ago. Unique results cannot be obtained for the star formation history over longer time baselines without better information on stellar metallicities and deeper photometry. The youngest model consistent with the data contains stars with constant metallicity of $Z = 0.001$ that mainly formed 2–4 Gyr ago. If stellar metallicity declines with increasing stellar age, then older ages are allowed of up to ≈ 8 Gyr. However, even at its peak of star-forming activity, the intermediate-age–dominated model for the Pegasus dwarf most likely remained relatively dim, with $M_V \approx -14$.

Key words: galaxies: dwarf — galaxies: irregular — galaxies: stellar content

1. INTRODUCTION

The Pegasus dwarf irregular galaxy (DIG) was first identified by A. Wilson (see Holmberg 1958), and its status as a nearby dwarf was confirmed only with the detection of H I by Fisher & Tully (1975). Despite its small size, Pegasus supports ongoing star formation, as evidenced by the presence of luminous blue stars (Hoessel & Mould 1982; Christian & Tully 1983; Sandage 1986) and small H II regions (Hunter, Hawley, & Gallagher 1993). Pegasus is fairly typical of the least luminous DIGs detected in the Local Group and a few other nearby galaxy groups (see Karachentseva et al. 1987; Miller 1996).

Pegasus presents an interesting structural combination of a dwarf irregular system, with a chaotic appearance due to star formation, and a relatively symmetric dwarf elliptical (dE) or dwarf spheroidal (dSph) galaxy, typically without young stars. Pegasus has a smooth outer envelope with elliptical isophotes and a brighter core that contains at least two OB associations (Ivanov 1996). It also has a relatively low amount of H I, as indicated by its moderate (for a DIG) ratio of $M_{\rm H\,I}/L_V = 0.4$ (Hoffman et al. 1996). Pegasus may, therefore, be a nearby example of a transition object between a dwarf galaxy dominated by current star formation and one dominated by past star formation.

While the evolution of very low mass galaxies is still unclear, one possibility is that brief epochs of very active star formation produce a significant fraction of the stellar

[1] Based on observations with the NASA/ESA *Hubble Space Telescope*, obtained at the Space Telescope Science Institute, which is operated by the Association of Universities for Research in Astronomy, Inc., under NASA contract NAS 5-26555.

TABLE 1

PROPERTIES OF THE PEGASUS DWARF IRREGULAR GALAXY

Property	Value	Reference
$E(B-V)$.....	0.15	1
B_T^0	12.61	2
$(B-V)_0$	$\approx$0.47	2
D (kpc)	760 ± 100	1
M_B.....	-11.8	1
M(H I) ($M_\odot$).....	3.1×10^6	3
M(H I)/L_B.....	0.4	
A_0 (kpc).....	1.7	4

REFERENCES.—(1) This paper; (2) NED; (3) Hoffman et al. 1996; (4) Holmberg 1958.

mass over a few dynamical timescales, or less than 1 Gyr (see, e.g., Babul & Ferguson 1996). Such events could disrupt or eject a small galaxy's interstellar medium (ISM), thereby inhibiting further star formation for a time (see, e.g., Dekel & Silk 1986; Sandage & Fomalant 1993; Marlowe et al. 1995). Under these conditions, much of the metal-rich supernova ejecta will also be lost, and so the remaining stellar populations are expected to be relatively metal-poor and may show little metal enrichment over time. It is interesting to see whether any indications exist for epochs of enhanced star formation activity in the recent history of the Pegasus dwarf, which might have led to its transitional morphological structure.

This paper presents the first optical study of the stellar population of the Pegasus dwarf based on observations obtained with the Wide Field Planetary Camera 2 (WFPC2) on the *Hubble Space Telescope* (*HST*). Supplementary ground-based data were obtained with the WIYN 3.5 m telescope.[2] The Pegasus dwarf is highly resolved into individual stars by WFPC2. These data sets allowed us to obtain high-quality color-magnitude diagrams (CMDs) for the Pegasus dwarf, which we analyze to derive its recent star formation history (SFH).

The next section reviews the global properties of Pegasus, and § 3 describes our new observations. Our analysis of the color-magnitude diagrams is covered in subsequent sections, the derived SFH is presented in § 7, and the results are summarized in § 8.

2. GLOBAL PROPERTIES OF THE PEGASUS DWARF IRREGULAR GALAXY

2.1. *Stellar Populations*

Table 1 summarizes several key observables for Pegasus. The $B-V$ color of Pegasus is sufficiently blue that some ongoing star formation is required. This is consistent with the CMD from an early CCD study by Hoessel & Mould (1982). They noted a modest young stellar population component and suggested that "recent star formation in Pegasus has been very subdued."

This point was reinforced by the discovery (Hunter et al. 1993) that Pegasus contains small, faint H II regions and some diffuse ionized gas (see also Aparicio & Gallart 1995; Skillman, Bomans, & Kobulnicky 1997).[3] Based on the Hunter et al. observed $L(\mathrm{H}\alpha) = 1 \times 10^{36}[D/(1\ \mathrm{Mpc})]^2$ ergs s^{-1}, we estimate that only a few late-type O stars have been born in the past few million years. This leads to a rough estimate of the current star formation rate (SFR_0) for a Salpeter initial mass function (IMF) of $\dot{M}_* \simeq 3 \times 10^{-4}\ M_\odot\ \mathrm{yr}^{-1}$, or $\mathrm{SFR}_0 \sim 500\ M_\odot\ \mathrm{kpc}^{-2}\ \mathrm{Myr}^{-1}$ averaged over the central region of the Pegasus dwarf. For a stellar mass of $M_* = 7 \times 10^6 M/L_V\ M_\odot$, the Roberts time to form the existing stars at the current SFR would be over 20 Gyr for the expected $M/L_V \geq 1$. The low $L(\mathrm{H}\alpha)$, lack of luminous blue stars, and $B-V$ color indicate that the SFR_0 is lower than the lifetime mean SFR for this galaxy.

More recently Aparicio & Gallart (1995) and Aparicio, Gallart, & Bertelli (1997a) made a ground-based study of Pegasus based on *VRI* photometry of resolved stars. They confirm the presence of young, evolved red stars. These are seen against an extensive background population of older stars on the red giant branch (RGB), which they suggest have ages of up to about 10 Gyr, and a range of possible SFHs are derived. However, CMDs obtained from ground-based observations are necessarily limited in precision and depth, because of image crowding. Stellar images observed with WFPC2 are typically 25 times smaller in angular area than those measured from the ground, even in excellent seeing. WFPC2 therefore yields more precise CMDs of the crowded stellar populations of galaxies, which are essential for constraining SFHs.

2.2. H I *and Kinematics*

Lo, Sargent, & Young (1993) mapped Pegasus with the Very Large Array (VLA) in the H I 21 cm line. Their maps show that the H I is concentrated within the core of the optical body of the galaxy, where several distinct clumps are present. The mean H I column density is $N(\mathrm{H\ I}) = 10^{21}$ cm^{-2}, and the peak values are at least twice the mean. The peaks roughly coincide with the region occupied by blue stars. A comparison with single-dish maps by Hoffman et al. (1996) shows that the Lo et al. VLA H I maps contain most of the H I flux; Pegasus does not appear to have an extended, massive reservoir of interstellar H I gas in an outer disk or halo.

2.3. H II *Regions and ISM Abundances*

Spectroscopy of the brightest H II region in Pegasus has been obtained by Skillman et al. (1997). The low-excitation spectrum shows strong [O II] λ3727 emission, and [O III] λ5007 emission is not detected. Using these data, Skillman et al. derive an abundance of $12 + \log(\mathrm{O/H}) = 7.9 \pm 0.1$–$0.2$ ($Z = 0.002$, or 10% solar), an oxygen abundance that is close to that of the Small Magellanic Cloud. Thus Pegasus appears to be surprisingly metal-rich relative to its blue luminosity. From the emission-line Balmer decrement, Skillman et al. derive an extinction of $E(B-V) = 0.2 \pm 0.1$, which is much larger than the $E(B-V) = 0.03$ predicted by the standard Galactic extinction model of Burstein & Heiles

[2] The WIYN Observatory is a joint facility of the University of Wisconsin–Madison, Indiana University, Yale University, and the National Optical Astronomy Observatories.

[3] A narrowband Hα image obtained with the WIYN telescope in 1997 August under good seeing conditions by Wisconsin graduate students A. Cole, J. C. Howk, & N. Homeier (1997, private communication) suggests that the second of the original H II regions is a background galaxy. These data also show that Pegasus contains several previously undetected faint, compact Hα sources that could be H II regions.

(1984). Reddening plays an important role in interpreting the CMDs of the Pegasus dwarf galaxy, and we discuss this issue in more detail in § 5.3.

3. OBSERVATIONS

3.1. *Observations with HST WFPC2*

Our WFPC2 data consist of three exposures of 600 s each in the F555W (V) and F814W (I) filters, and a set of 2 × 900 s and 2 × 1100 s exposures in the F439W (B) filter. Each image is offset by a few pixels plus a fractional pixel offset, or "dithered" (Leitherer 1995; Fruchter & Hook 1997), with respect to each other in an attempt to compensate for the undersampled point-spread function of WFPC2. The images in each filter were first registered to the nearest integer pixel, and then cosmic-ray–cleaned and combined using techniques described by Saha et al. (1996). The nominal pointing was to $\alpha = 23^{h}28^{m}33^{s}.0$, $\delta = +14°44'6''.0$ (J2000.0) at the WFALL-FIX aperture, which is located approximately 8″ along the diagonal running from the center of the WFPC2 field to the corner of the WF3 camera. The resulting WFPC2 V image of the heart of Pegasus is shown in Figure 1, with a close-up view in Figure 2.

Photometry was carried out on the combined images using a version of DoPHOT (Schechter, Mateo, & Saha 1993) altered to take into account the special circumstances presented by undersampled WFPC2 images, which also contain variable point-spread functions (Saha et al. 1996). The photometry was calibrated and converted to the "standard" BVI system using the precepts laid out in Holtzman et al. (1995). Independent analysis of the images indicates zero-point uncertainties of ± 0.05 mag in V and less than ± 0.03 mag in $V-I$. We therefore adopted these values as our minimum photometric errors. The B-band data show larger scatter, reflecting their lower signal-to-noise ratios. The resulting color-magnitude diagrams are presented in Figures 3 and 4 for the individual WFPC2 CCDs, and for the combined data in Figure 5. Figure 6 displays the internal photometric error distributions. The properties of these CMDs are described in § 4.

3.2. *Ground-Based Observations with the WIYN Telescope*

CCD images in the V and I filters were obtained in 1996 September with the WIYN 3.5 m telescope. The field of view of the 2048 × 2048 pixel CCD is 6′.7 at a scale of 0″.2 pixel^{-1}. The exposure times were 600 s in I and 500 s in V.

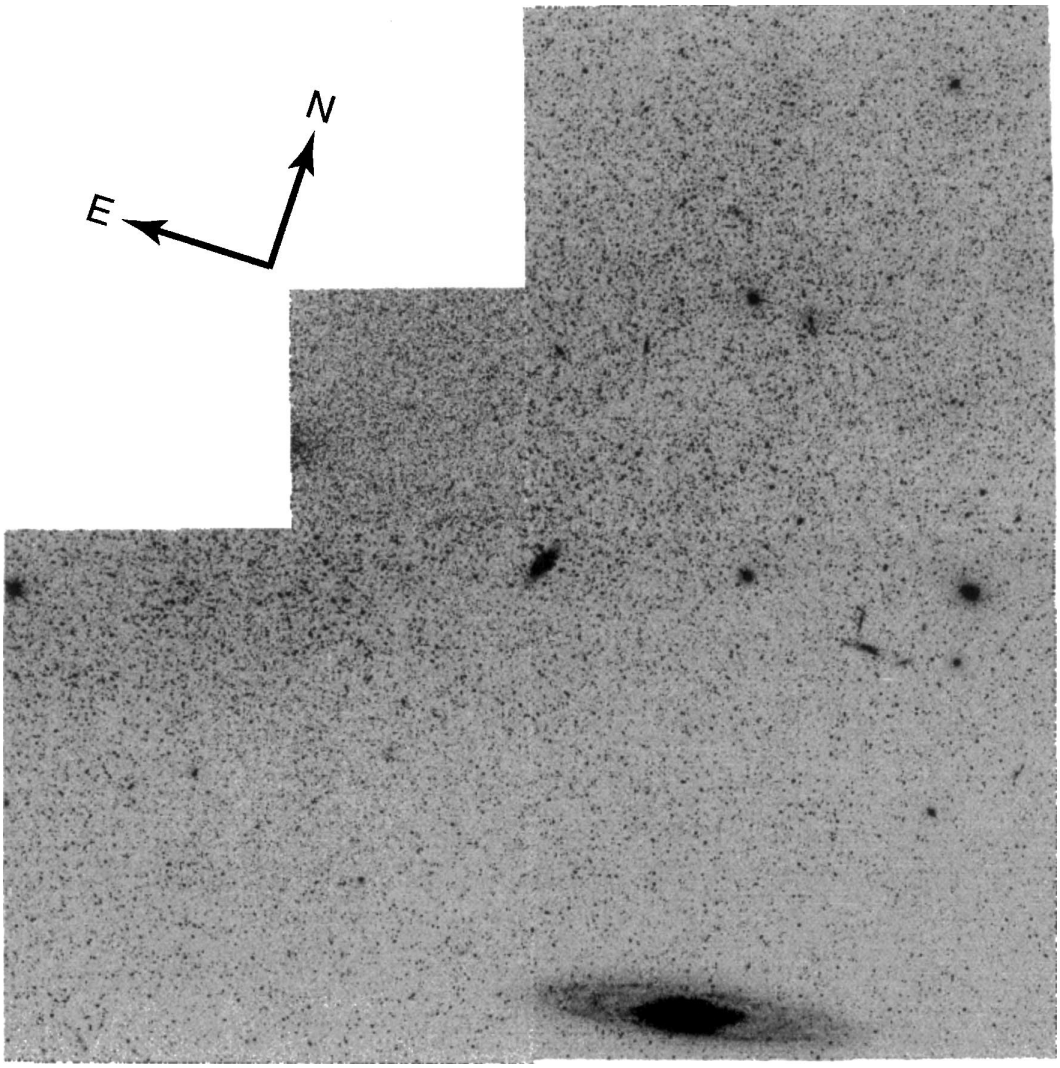

FIG. 1.—Mosaic of the WFPC2 F555W (V) image of the central regions of the Pegasus dwarf irregular galaxy. This galaxy is highly resolved by WFPC2, and crowding is not a major factor in the photometric accuracy. Note that several background galaxies are visible; evidently Pegasus is obscuring a relatively rich group of more distant galaxies.

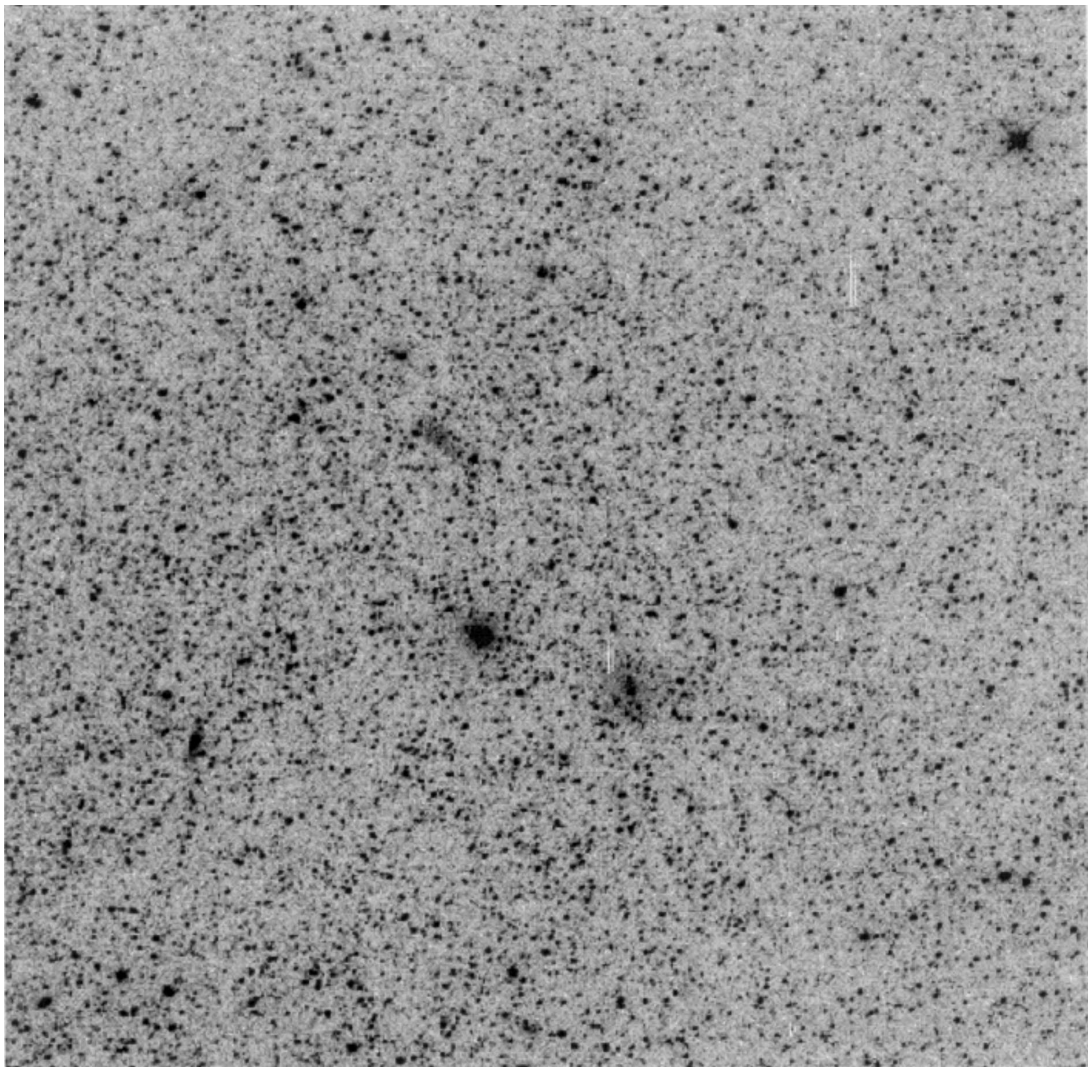

FIG. 2.—Section of the WFPC2 F555W image of the Pegasus dwarf galaxy from the WF4 camera. This detail of the data illustrates the low stellar densities at our magnitude limit and the high visibility of background galaxies seen through the Pegasus dwarf.

Conditions were clear around Pegasus but deteriorating elsewhere in the sky during our observations; we cannot be sure of our photometric zero points because of the possible presence of clouds. The FWHM image sizes were $\approx 0\farcs6$.

These images were processed in a standard way with IRAF.[4] Transformations to standard magnitudes were approximated by matching our WFPC2 results. The WIYN telescope V-band image is shown in Figure 7. Results of our DoPHOT photometry of the WIYN images are displayed in Figure 8. The main sequence (MS) is more scattered and the RGB is broader in color in Figure 8 than in the *HST* CMD in Figure 4, consistent with the expected effects from crowded ground-based images. There is also a larger population of bright red ($I < 21$ and $V-I > 1.5$) stars, on the extended asymptotic giant branch (AGB), which the WIYN data show extend beyond the radius in the Pegasus dwarf covered by our WFPC2 images.

[4] IRAF is distributed by the National Optical Astronomy Observatories, which are operated by the Association of Universities for Research in Astronomy, Inc., under cooperative agreement with the National Science Foundation.

4. COLOR-MAGNITUDE DIAGRAMS

4.1. *Description of Major Features*

A sparsely populated "blue plume" of well-resolved stars is present in our CMDs and is best defined in the WFPC2 (V, $B-V$) CMD in Figure 3. It consists of an MS with adjacent core helium burning (HeB) evolved intermediate-mass stars that form the "blue loop."

The straight, nearly vertical structure of the MS indicates that the hotter young stars in the Pegasus dwarf have spectral classes of A or earlier; at later spectral types, the MS changes to a flatter slope where color varies more rapidly with luminosity (cf. the Large Magellanic Cloud field observed by Gallagher et al. 1996). We can obtain an idea of the recent SFH through comparisons with other nearby star-forming galaxies observed with WFPC2, such as the Magellanic Clouds (Gallagher et al. 1996; Holtzman et al. 1997), Sextans A (Dohm-Palmer et al. 1997a, 1997b), and Leo A (Tolstoy et al. 1998). These confirm that even by the standards of low surface brightness dwarf irregular galaxies, Pegasus has a relatively small population of young stars.

The dominant feature of the (I, $V-I$) CMD (Fig. 5) is the populous "red plume," consisting of the RGB and a dense

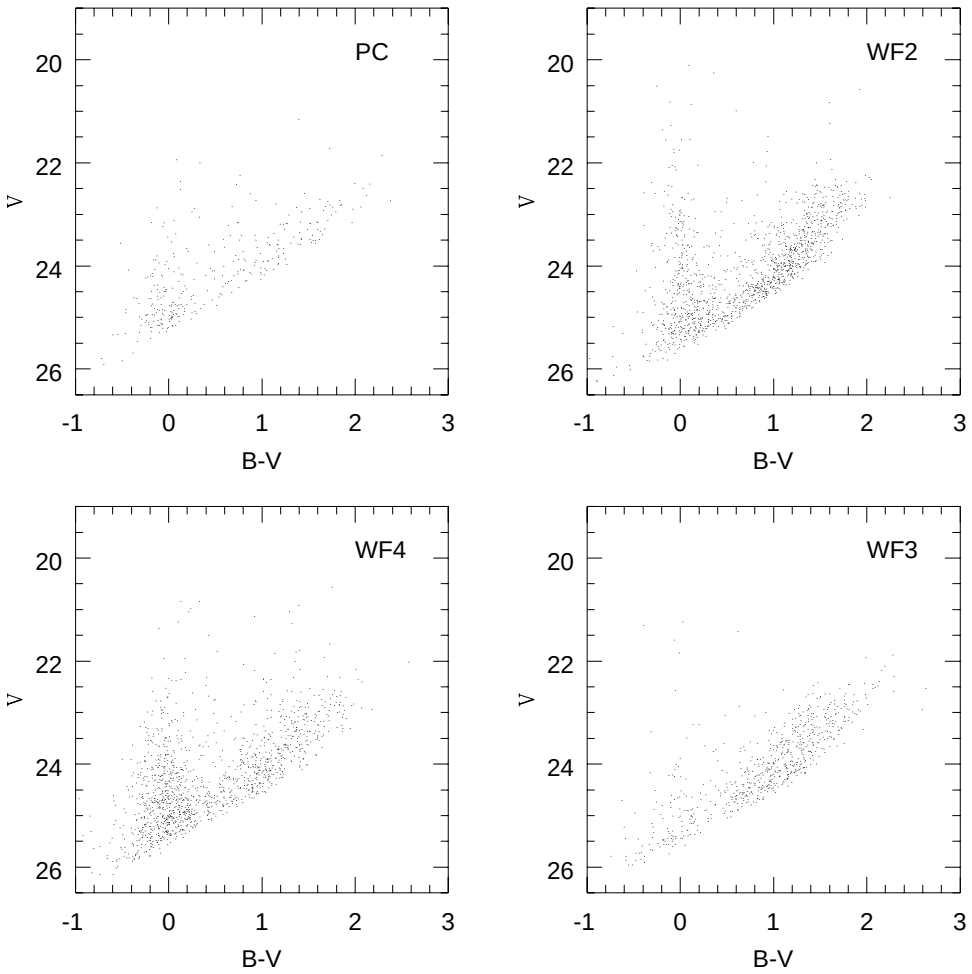

FIG. 3.—Observed color-magnitude diagrams for the Pegasus dwarf galaxy for each of the four WFPC2 CCDs in terms of V magnitude and $B-V$ color

concentration of core helium burning stars in the red clump (RC) overlying the lower RGB. In addition, we see members of an extended AGB population, and this is confirmed in the larger field WIYN data (see also Aparicio et al. 1997a). A few red supergiant (RSG) stars are likely present, with colors of $V-I \approx 1$ and $I < 21$. In the blue the RGB is spread in color and not well measured at the depth reached by our WFPC2 data. This part of our CMD resembles the WFPC2 observations of the Local Group dE galaxy NGC 147 (Han et al. 1997). The RGB and the RC are prominent in both galaxies (see Fig. 9), which is surprising, given their very different morphological classes. The obvious differences between the CMDs of the two galaxies are the horizontal branch (HB), which is seen in NGC 147 but not in the shallower Pegasus WFPC2 images; the greater color width of the RGB in NGC 147; the sharp RGB tip in NGC 147; and the presence of young stars in Pegasus. The older stellar population appears to be more complex in terms of its range of ages and metallicities in NGC 147 than in Pegasus, but star formation has persisted for a longer time in the smaller Pegasus system.

4.2. *Spatial Distributions*

Spatial density distributions of stars also provide a means to explore the SFH of galaxies. For example, it is standard practice to use OB stars as markers of recent star formation, and this philosophy can be readily extended to less luminous main-sequence stars to investigate stellar age–spatial distribution correlations in galaxies. Additional insights into the SFH are sometimes supplied by star clusters, whose ages can be reasonably well determined from colors when they are less than a few gigayears old (see, e.g., Hodge 1980).

Unfortunately, in the region of the Pegasus dwarf covered by WFPC2 we find only one-half of a moderately dense star cluster. Possible star clusters were noted by Hoessel & Mould (1982). The WFPC2 images show that the Pegasus dwarf is in front of a moderately rich group of galaxies, and some of these background galaxies could have been mistaken for star clusters in ground-based images. However, the central star cluster is partially in our PC image, and has a diameter of ≈ 40 pc with a moderate stellar density enhancement over the surrounding field. We attempted to make a CMD for this cluster, but it is of poor quality because of crowding, and otherwise indistinguishable from the surrounding field. The cluster appears to have a strong RC and RGB with no definite MS stars; thus it is probably an intermediate-age object, older than about 2 Gyr. A deeper observation, including the entire cluster, could yield a more accurate cluster CMD and allow a better age estimate.

While the connections between SFRs and star cluster formation rates remain obscure, very dense, luminous "super star clusters" are often produced in small galaxies during starbursts (Meurer et al. 1992; O'Connell, Gallagher,

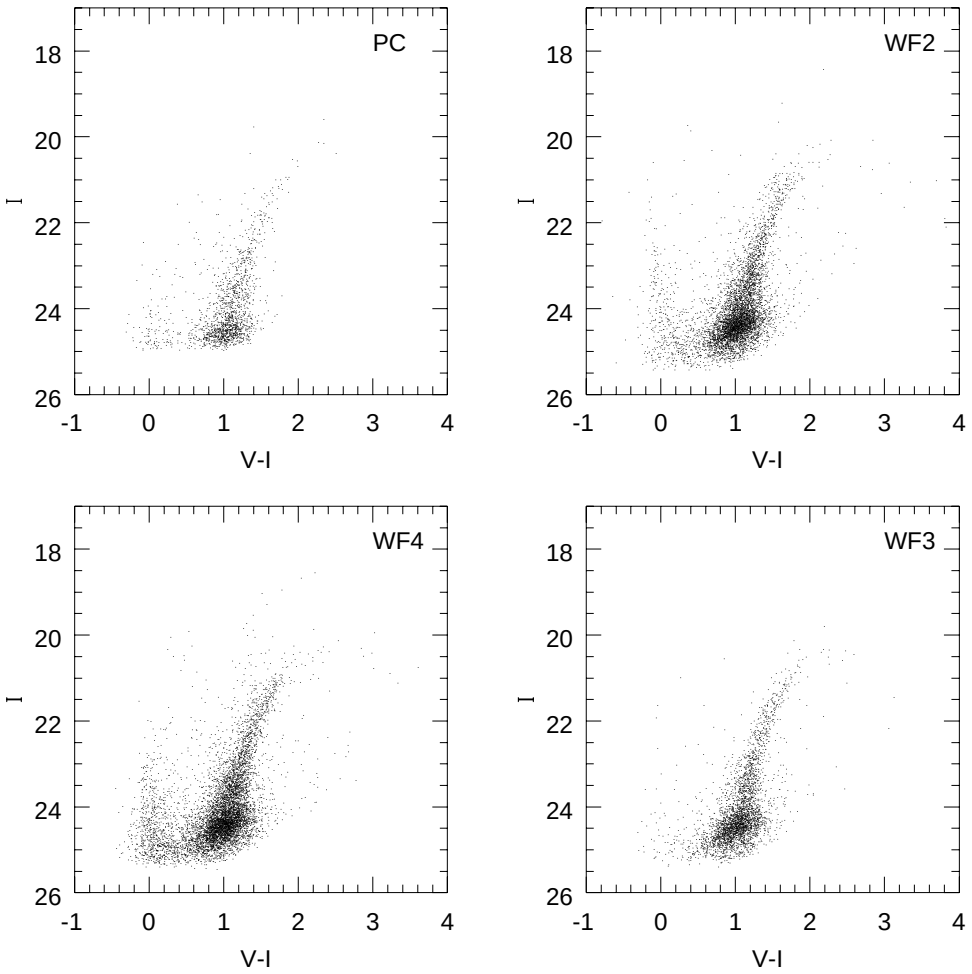

FIG. 4.—Same as Fig. 3, but for I and $V-I$

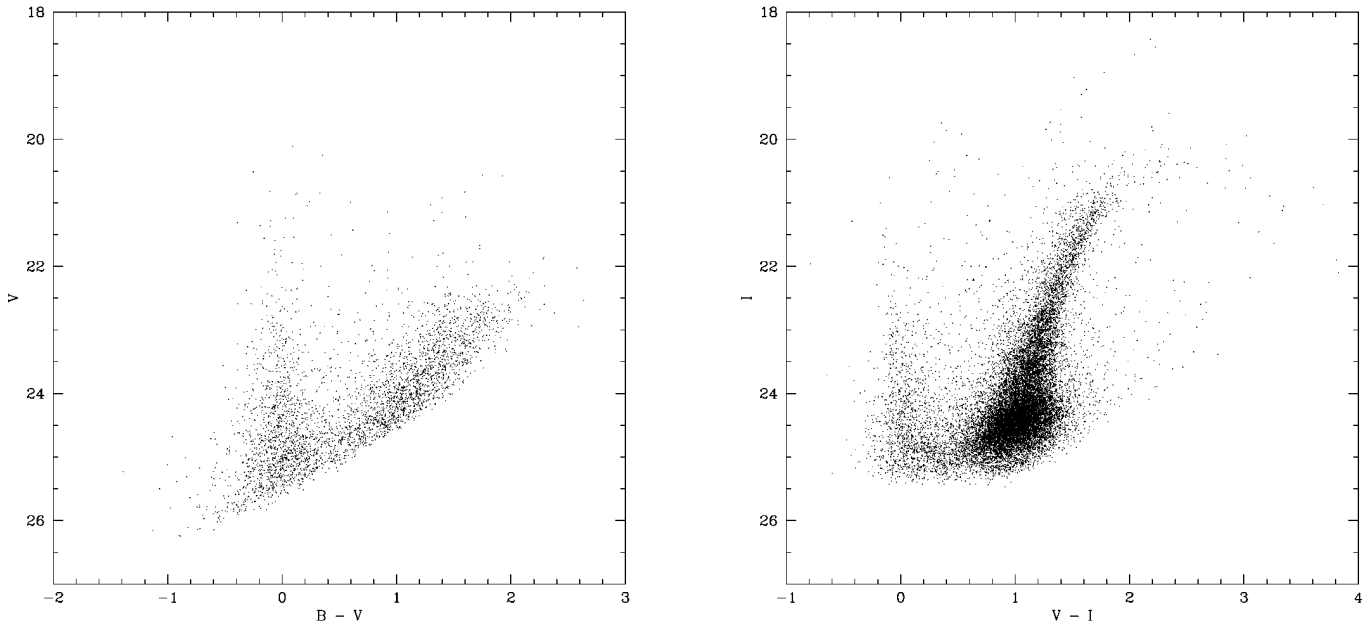

FIG. 5.—Combined (V, $B-V$) (*left*) and (I, $V-I$) (*right*) color-magnitude diagrams derived from the WFPC2 data sets. These data are the basis of our analysis of the SFH of the Pegasus dwarf galaxy.

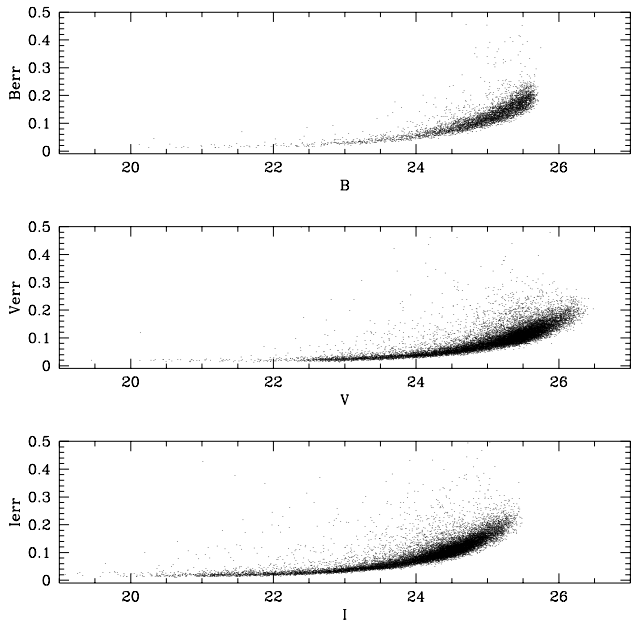

FIG. 6.—Photometric errors for each of the three bands for the WF CCDs, which contain most of the measured stars.

& Hunter 1994). These types of clusters would be denser and richer than the Pegasus central star cluster. The absence of candidate super–star clusters in Pegasus is consistent with models in which no starburst occurred during at least the past few gigayears, this timescale being set by the likely minimum dynamical lifetimes for dense star clusters to dissolve (Goodwin 1997).

The general pattern in all nearby galaxies is for younger stars to clump into associations, although examples of young, massive stars in the field also exist (see, e.g., Massey 1998). Stellar associations drift apart with velocities of a few kilometers per second, and former members will diffuse within a galactic disk; the mixing times of stars within the disks of galaxies are typically ≤ 1 Gyr (see § 5.1 in Gallagher et al. 1996). In addition, the region of a galaxy that is accessible to stars born in a disk may be bounded by the energy and angular momentum of their parent interstellar gas clouds. Thus, stars formed from interstellar clouds near the center of a galaxy are unlikely to have sufficient energy or angular momentum to travel very far out in a stellar disk.

Stellar surface density distributions derived from our WFPC2 images of the Pegasus dwarf are shown in Figure 10. The stellar populations in the Pegasus dwarf show the expected trend for most of the younger stars to be spatially clumped, and the older stars to be more smoothly distributed. Figure 10*a* illustrates the surface densities of young stars located in the blue plume from the $(V, B-V)$ CMD in Figure 5 (*left*). These stars are in two major concentrations that resemble diffuse OB associations (Ivanov 1996), and are located near the center of the optical galaxy. As shown in Figure 10*b*, the RGB and RC stars are more symmetrically distributed about the central star-forming zone.

Figure 10*c* presents the density of extended-AGB stars derived from the WIYN CCD images. We find good agreement between the surface densities of extended-AGB stars measured in the WFPC2 images and from WIYN; we therefore prefer the wide field of view of the WIYN images for this plot. The densest concentration of extended-AGB stars is found along the major axis, following approximately the same pattern as is seen in all of the other stars. Exterior to this zone the distribution of extended-AGB stars is lumpy; we may, therefore, be seeing remnants of older star-forming regions or the modulation of apparent stellar densities by dust within the Pegasus dwarf. The outermost regions appear as discrete clumps because of statistical fluctuations.

5. INGREDIENTS FOR MODELING THE CMD

5.1. *Stellar Evolution Models*

Stellar evolutionary tracks give the luminosity, effective temperature, and surface gravity for single stars of a given mass and chemical composition as a function of age. The tracks depend on basic astrophysical parameters, such as the initial mass, metallicity level, and distribution. The properties of real stellar populations also depend on a variety of properties not explicitly included in most current stellar evolution models, such as stellar rotation rates and the presence of close binary companions. The results from numerical calculations are also sensitive to the treatment of convection in terms of the ratio of pressure scale height to convection scale and to the effect of convective core overshoot.

In this paper we primarily use two sets of stellar evolutionary tracks at $Z = 0.004$ and $Z = 0.001$ computed by the Geneva group (Charbonnel et al. 1993; Schaller et al. 1992), which we compare with the tracks given by the Padua group stellar evolution models (Fagotto et al. 1994). In order to most accurately compare the two sets of model tracks, it is necessary to work from a uniform set of equivalent evolutionary points (EEPs). We chose to use the EEPs defined by Schaller et al. (1992). These points are defined differently during the various phases of stellar evolution. For example, on the main sequence, the EEPs represent a sequence of decreasing central hydrogen abundance. The EEPs must be carefully chosen so as to properly sample all of the color-magnitude space spanned by the tracks. This ensures the ability to correctly model, e.g, the "bump" in the RGB luminosity function, or the main-sequence "hook" exhibited by stars with convective cores.

In converting the Padua tracks to the Geneva EEPs, we carefully interpolated the tabulated values of $\log L$, $\log T_{\rm eff}$, and age at the given points to the appropriate values at the EEPs. Along each Padua track we identified the 51 Geneva EEPs and interpolated new tracks between these points using a cubic spline. The accuracy of this process was checked by overplotting the original and converted tracks; the differences were found to be negligible. This allows us to properly interpolate when producing stellar population models, as discussed by Tolstoy (1996). While we do not explicitly include binary stars in our models, we do allow for a population of outlying stars to be present, which effectively account for binary star blends in our data.

The two sets of stellar evolution models differ in several details, as can be seen in Figure 11, where we plot the 1.5 and 2 $M_\odot$ stellar evolutionary tracks from Padua (*solid lines*) and Geneva (*dashed lines*). The RGB tip luminosity differs by more than 0.5 mag, and on the upper part of the RGB, the Padua tracks are frequently several tenths of a magnitude bluer than the Geneva tracks. These differences are probably the result of the treatment of convective overshoot or the exact definition of the point where the helium

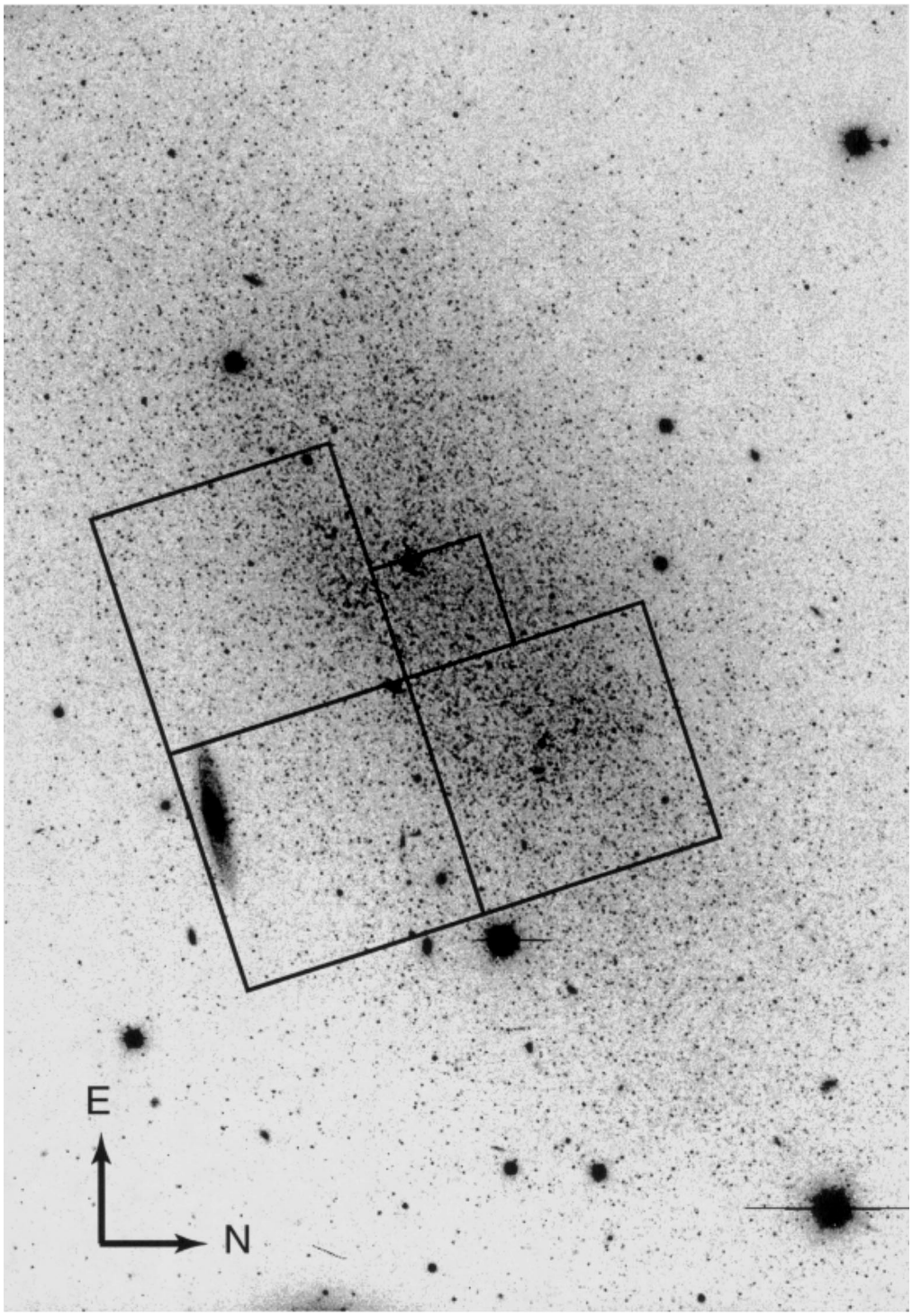

FIG. 7.—Pegasus observed in the *V*-band with the WIYN 3.5 m telescope shows the bright core where star formation is occurring, and the more extended dE-like main body of the galaxy. Extended-AGB stars and the more luminous RGB members are well resolved over much of the galaxy in this 0.″6 seeing image. Our field of view is 6.′7 on a side, corresponding to 1.5 kpc for a distance of 760 kpc. The location of the WFPC2 observations is also shown.

flash occurs and the RGB models are terminated. The agreement between the tracks is better along the MS and at the base of the RGB. Therefore, if we used Padua rather than Geneva stellar evolutionary tracks, we would find a slightly larger distance and a younger (or more metal-poor, or both) stellar population.

The *numbers* of stars predicted to exist at any location off of the zero-age MS for the same SFH also differs for Padua and Geneva stellar evolution models. This occurs because at a given initial mass, the Padua stellar models are generally more luminous and also have longer lifetimes. The IMF requires that the numbers of stars born per unit stellar mass will increase as stellar mass decreases. For a given SFR, the Padua tracks will predict more stars at each luminosity (after the zero-age MS) than the Geneva tracks. As a result, the SFR derived from an observed CMD will be somewhat lower for Padua models than for the Geneva models.

Because most galaxies have complex SFHs, the many interconnected effects that determine the properties of a galactic CMD come into play. The history of a galaxy can

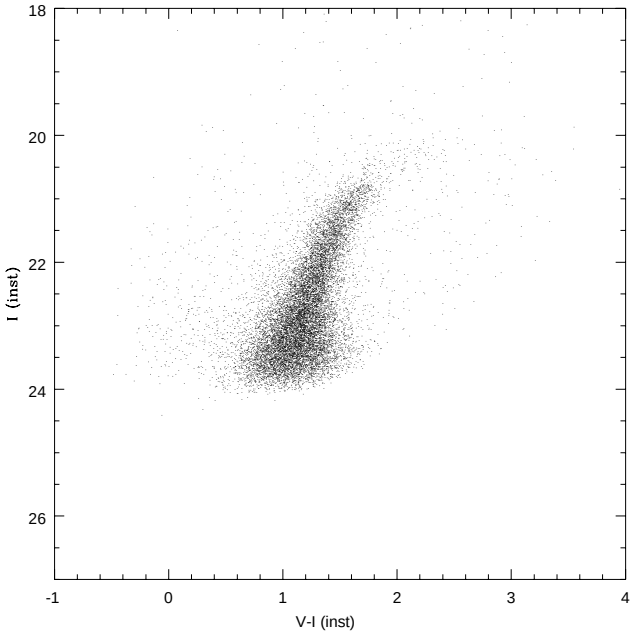

FIG. 8.—Color-magnitude diagram in the instrumental I and $V-I$ colors from photometry of stars in our WIYN images. These data have been approximately transformed to standard magnitudes using our WFPC2 results.

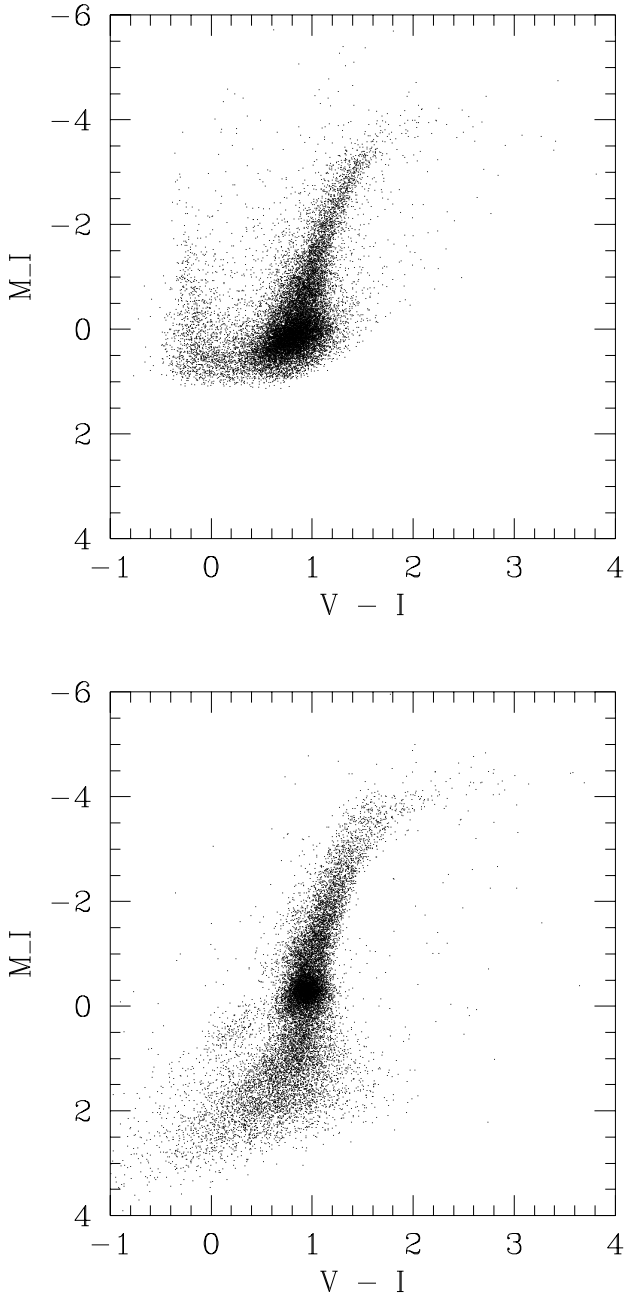

FIG. 9.—*Top*, Pegasus (I, $V-I$) CMD; the NGC 147 outer field WFPC2 (I, $V-I$) CMD from Han et al. (1997) is shown for comparison (*bottom*).

therefore be effectively modeled using numerical (e.g., Monte Carlo) simulations, in which a composite stellar population is randomly extracted from theoretical stellar evolutionary tracks using an assumed IMF and SFH. We followed the approach described in detail by Tolstoy (1996), and made a number of simulated CMDs for a variety of assumed SFHs. Each simulation then depends upon *all* the main parameters that determine an observed CMD, unlike the standard isochrone-fitting methods previously used. Monte Carlo simulations were first used to simulate galactic CMDs by Tosi, Greggio, and collaborators (e.g., Tosi et al. 1991), and these ideas were further developed by Tolstoy & Saha (1996) and Tolstoy (1996) to allow statistical comparisons between many different CMD models and the multiple-color photometric data sets.

Using the techniques of Tolstoy & Saha (1996), we created stellar population models for a variety of potentially feasible SFHs using Geneva stellar evolutionary tracks. These are comparatively well defined for the recent history of the Pegasus dwarf, but become nonunique at ages beyond about 2 Gyr. We then determined the most likely SFH to match our observed CMD for the Pegasus dwarf. Our method allows for limitations in the data, such as the increasing scatter and rising incompleteness at fainter magnitudes, which preclude finding a unique solution for the SFH of Pegasus based on our current data sets.

5.2. *Matching the Observational Errors*

The two main observational effects that we must incorporate into our model CMDs before we can accurately compare them with observed CMDs are observational errors (plotted in Fig. 6), and the incompleteness, or the number of stars we miss at given observed magnitude range because of crowding or noise (see Tolstoy 1996). Because our *HST* images are effectively uncrowded, the incompleteness is very well correlated with the observational errors. This issue has been studied for Sextans A in detail by Dohm-Palmer et al. (1997a), and we use these results in our models.

5.3. *Extinction*

The standard Galactic extinction to the Pegasus dwarf derived by Burstein & Heiles (1984) is small, $E(B-V) = 0.03$. However, our observations show that with this extinction correction, the Pegasus dwarf's MS is too red in $B-V$ and $V-I$; we could find no models with low reddening that would simultaneously fit in both colors. We

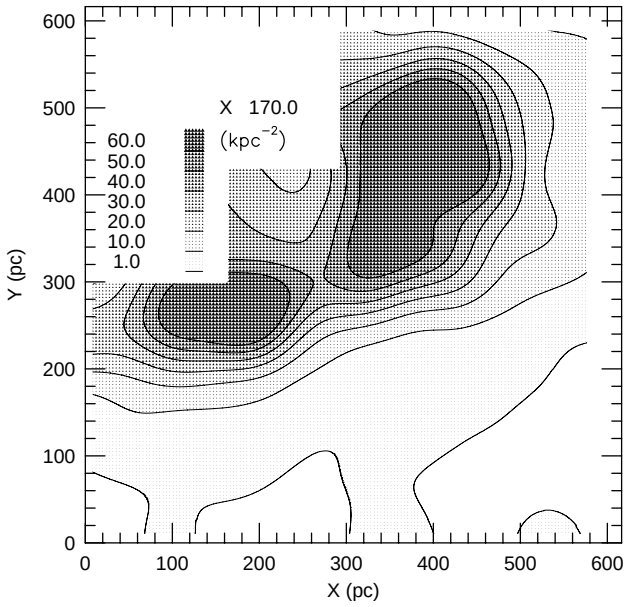

FIG. 10*a*

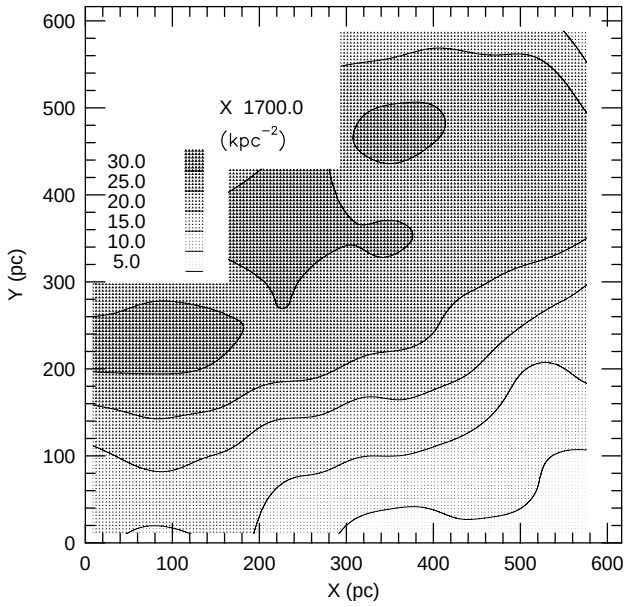

FIG. 10*b*

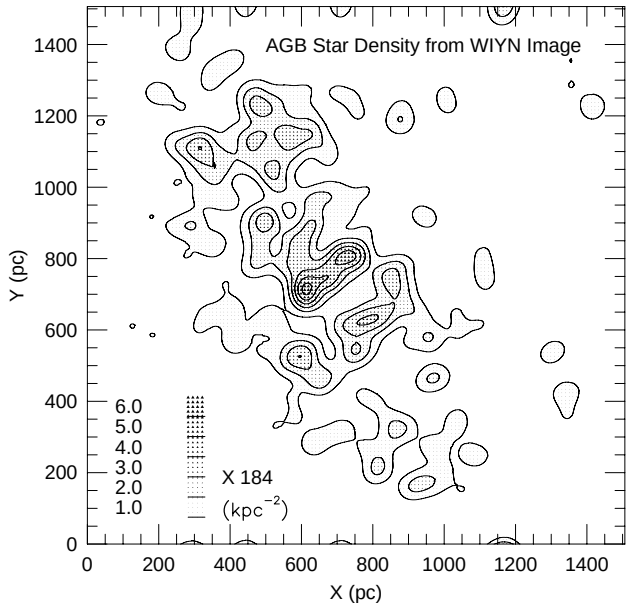

FIG. 10*c*

FIG. 10.—(*a*) Projected densities of stars selected from different regions of our WFPC2 CMDs. This diagram provides densities of younger stars on the main sequence and in core helium burning evolutionary stages within an 8″ smoothing region. (*b*) Same as (*a*), but showing the locations of RGB stars, which are less centrally concentrated than the younger stars. (*c*) Density plot for extended-AGB stars derived from our WIYN data, with the same orientation as Fig. 7. It was made with the same smoothing scale used for the WFPC2 density plots and shows a relatively clumpy distribution of AGB stars in the inner galaxy. Poor statistics produced low-amplitude features in the outer parts of the galaxy. Note that the star-forming region is offset with respect to the distribution of AGB stars.

made a model $B-V$ versus $V-I$ two-color diagram and empirically derived a possible range of reddenings (and distances, with which it is weakly correlated). Feasible reddening values were identified by requiring the model and observed MS to agree to within ± 0.05 mag in both $B-V$ and $V-I$ colors. This result is almost independent of our choice of abundance or recent SFH, since it depends only on the almost invariant optical colors of the upper main sequence. We also required fits at the 0.2 mag level to the RGB tip and to the RC, while avoiding producing CMD features that are *not* seen, such as an extended blue loop. We thus find $E(B-V) = 0.15 \pm 0.05$ from model fits to our WFPC2 *BVI* CMDs.

To check the consistency of this reddening derived from the CMDs, we redetermined the mean Galactic extinction *toward* Pegasus by converting the Galactic H I column density to an extinction. For this test, we took $N(\mathrm{H\ I}) = 3.7 \times 10^{20}$ cm^{-2} derived from an H I spectrum recently taken by P. Kalberla (1997, private communication) with the Effelsberg 100 m radio telescope, which has a 9′ beam size. Following Diplas & Savage (1994), we find that $E(B-V) = 0.08$ is predicted for a standard Galactic dust-

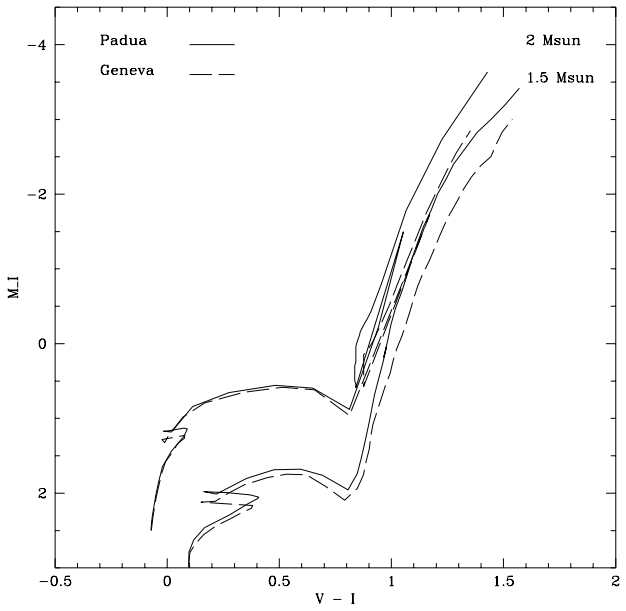

FIG. 11.—Comparison of Geneva and Padua stellar evolution tracks. The Padua models were interpolated to the same equivalent evolutionary points as were used to make the Geneva tracks. Note the offset between the RGB tip locations for these two sets of models.

to-gas ratio. The *internal* extinction within Pegasus should be low (Fitzpatrick 1985), unless the mean N(H I) is severely underestimated. Using the Lo et al. average N(H I) within Pegasus, the internal extinction for an SMC dust-to-gas ratio would be $E(B-V) \leq 0.03$ from the H I data. We therefore estimate a total extinction of about $E(B-V) \approx 0.1$ from the measured N(H I).

Additional information comes from the *IRAS* 60 μm and 100 μm full-resolution co-added (FRESCO) maps of the region around Pegasus. If there is a large amount of far-infrared (FIR) (100 μm excess) cirrus in front of Pegasus, the H I observations could underestimate the Galactic extinction. The 100 μm *IRAS* map is shown in Figure 12, where we see a small FIR excess at the position of Pegasus. The 100 μm/60 μm ratio is consistent with the more general infrared cirrus in this field; this is not a dust-free direction. A quantitative estimate of the extinction from the *IRAS* data can be made following the approach of Laureijs, Helou, & Clark (1994). For a peak 100 μm brightness of 0.4 Jy sr^{-1} averaged over the $\approx 6'$ effective resolution of the *IRAS* map, the predicted extinction is $A_B = 0.03$ mag. However, we might expect this to be an underestimate if the dust is far from the heating sources in the Galactic disk and, therefore, cold and radiating inefficiently in the *IRAS* 100 μm band. The high 60 μm/100 μm ratio of the dust toward Pegasus supports this possibility.

The estimators for foreground Galactic extinction toward the Pegasus dwarf do not yield consistent values and, furthermore, are averages over larger angular scales than the size of the WFPC2 field of view. Since we are working from CMDs, our data require a larger extinction than the Burstein & Heiles value. We therefore adopt $E(B-V) = 0.15$ for the remainder of this paper and apply this extinction to all of our data: $A_B = 0.62$, $A_V = 0.47$, and $A_I = 0.28$.

5.4. *Distance*

The distance to the Pegasus DIG has not been independently established from well-calibrated standard candles, such as Cepheid or RR Lyrae variable stars. Hoessel et al. (1993) reported the detection of what appeared to be Cepheid variable stars in Pegasus from a series of CCD images taken in the Thuan-Gunn r band. Their distance modulus was $(m-M)_0 = 26.2$, corresponding to $D = 1.7$ Mpc. Aparicio (1994) showed the Hoessel et al. candidate Cepheids to have the red colors of stars associated with the RGB. Photometry from our WIYN images agrees with his conclusion; the "Cepheids" are some other class of red variable star, and the Cepheid distance is not valid. Aparicio derived a revised distance modulus of $(m-M)_0 = 24.9 \pm 0.1$, or $D = 960$ kpc, from the location of the RGB tip following the calibration of Lee, Freedman, & Madore (1993a), under the assumptions of small extinction and that stars with ages of over 2 Gyr dominate the RGB. Our analysis suggests that a modest further reduction in distance is now required to account for increased extinction and a mix of stellar population ages, as discussed below.

The Pegasus dwarf has also played a role in efforts to obtain distances from luminous stars. Sandage (1986) used Pegasus as one of his calibrators in exploring the relationship between stellar and parent galaxy luminosities. This approach was extended by Rozanski & Rowan-Robinson (1994), who found $(m-M)_0 = 27.6$. However, the recent level of star-forming activity should be a key factor in determining the luminosity distribution of massive young stars in galaxies. Because Pegasus has a depressed SFR_0, it is likely that the most-luminous-stars method will overestimate the distance, as is the case for Pegasus.

In our *HST* CMDs for Pegasus, there are no unique features from which an accurate distance can be unambiguously obtained, such as a blue HB with a narrow luminosity distribution. The shape of the MS and blue loop somewhat constrain the distance to Pegasus. If the distance were $(m-M)_0 > 26$, then the mass function would make blue core HeB stars hard to avoid in larger numbers at the top of blue plume than are observed. If $(m-M)_0 < 23$, then we would expect to see a change in slope of the MS as radiative cores and convective envelopes appear in lower mass MS stars.

The luminosity of the RGB tip and the RC further constrain the range of possible distances to Pegasus. However, because young and intermediate-age stellar populations are present, the luminosity of the RGB tip can be uncertain (Lee et al. 1993a; Saha et al. 1996). RGB tip stars on the second ascent of the RGB during their AGB phase can extend the observed RGB tip and make the galaxy appear farther away. The RC luminosity decreases slowly with age (Lattanzio 1991), which makes it an inaccurate distance estimator by itself, although it is useful as a consistency check. Therefore, by reducing the distance to Pegasus, we increase the age of stars in the RC. By comparison with NGC 147, whose distance is reliably measured by Han et al. (1997) from the location of the HB (see Fig. 9), the range of distances for the Pegasus dwarf consistent with the luminosities of its RGB tip and RC are $24.2 \leq (m-M)_0 \leq 24.6$.

There is no reasonable reddening that can be combined with distances of $(m-M)_0 \geq 24.6$ to yield an acceptable match to the observed WFPC2 *BVI* color-color diagram for Pegasus. Note that in some cases we could obtain a fit for either the *BV* or *VI* CMDs, but the same reddening did not fit both diagrams simultaneously. Thus reddening and distance are correlated, and observations in three or more filters are essential in cases where we must derive both a

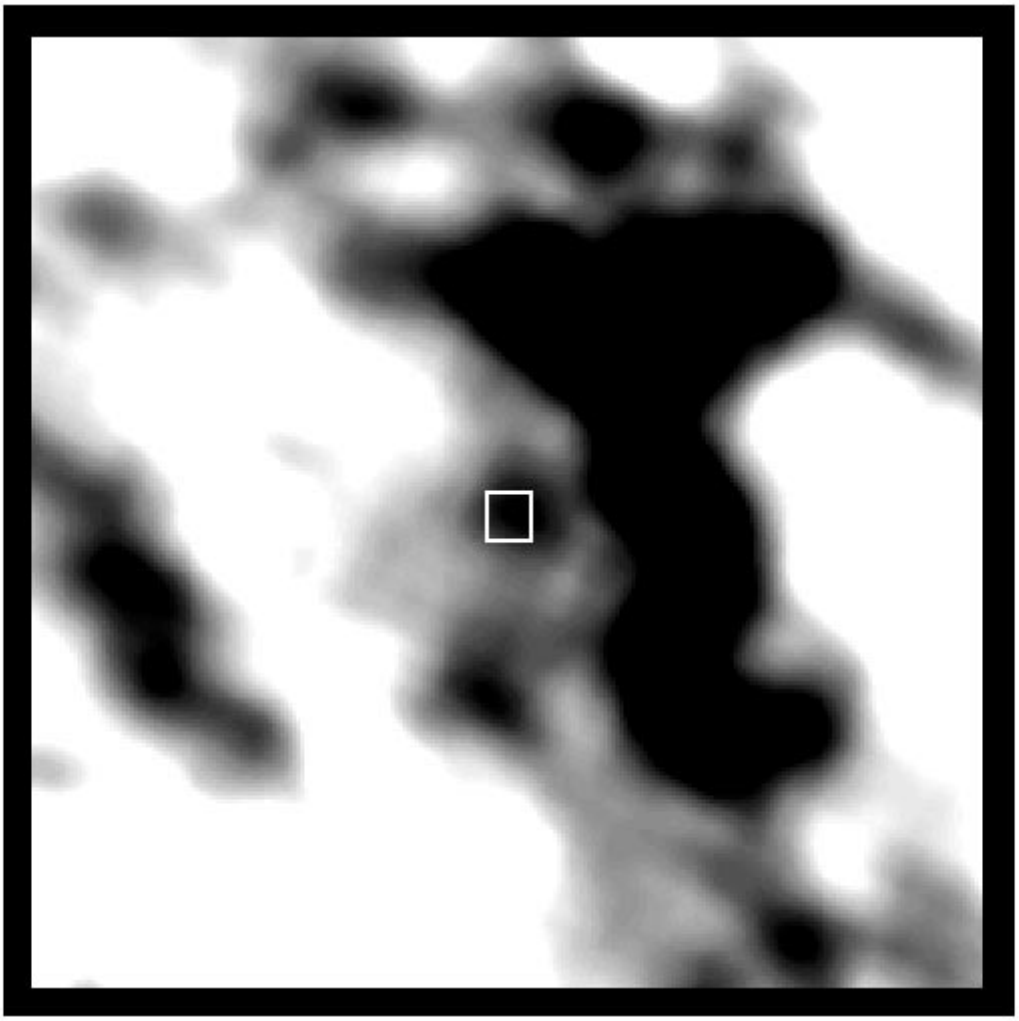

FIG. 12.—*IRAS* 100 μm map of a region centered on the Pegasus dwarf, marked by the small box. The field is 1° square, with 15 arcmin^2 pixels

distance and reddening to a galaxy from a CMD (see also § 5.3).

Therefore, we find and adopt a new distance of $(m - M)_0 = 24.4 \pm 0.2$, or $D = 760 \pm 100$ kpc, to Pegasus. Most of this change, compared with the larger distance of Aparicio (1994), is the result of our assumption of nearly 0.3 mag more I-band extinction. Our revised distance suggests that Pegasus is a member of the M31 "family" within the Local Group (Karachentsev 1996).

5.5. *Metallicity*

For the initial discussion in this paper, we set the metallicity of the whole stellar population in Pegasus to be equal to that of the youngest stars. We are reasonably confident in our choice of the $Z = 0.001$ models to represent the younger stars in Pegasus over higher metallicities because of the presence of stars between the MS and RGB. These should be mainly stars in core HeB, blue-loop evolutionary phases, despite the absence of a well-defined "blue loop" morphology. This is probably a result of small number statistics and is also consistent with the O abundance measured for the brightest H II region in Pegasus.

We have no data to measure the metallicities of the intermediate-age or older stars that make up the RGB. Such measurements require the detection of an HB, extension of our photometry over a longer color baseline (e.g., into the infrared), use of narrower band filters, or spectroscopy of a statistically complete sample of RGB stars. We can only say that most of the RGB stars are unlikely to be much lower in metallicity than the $\approx 1/20$ solar value we assume for young stars, or the RGB would be both narrow and blue, as in the Carina dSph galaxy (Smecker-Hane et al. 1994; Da Costa 1998). This is clearly not the case in the Pegasus dwarf.

Our SFH models therefore assume that the stellar metallicity levels have remained approximately constant at $Z = 0.001$ over most of the life of the Pegasus dwarf. Additional support for this assumption comes from theoretical models of dwarf galaxy evolution (e.g., Mori et al. 1997; Ferrara & Tolstoy 1998; Hensler, Gallagher, & Theis 1998). These predict a rapid initial metal enrichment at the epoch of formation of the galaxy, followed by a plateau. Hence the assumption of zero metallicity evolution over most of the lifetime of these small systems could be reasonable. Our model for the Pegasus dwarf is more metal-poor than the evolving-metallicity SFH models presented by Aparicio et al. (1997a). If there is significant metallicity evolution in Pegasus, such that metallicity substantially declines with

increasing stellar age, then we will overestimate the metallicity for the older stars seen on RGB and thus underestimate their ages.

6. RECENT STAR FORMATION HISTORY

Having determined all the initial conditions for our models, we now turn to finding an SFH model that best matches our data. Model CMDs that might represent Local Group dwarf irregular galaxies when observed with WFPC2 have been calculated by Aparicio et al. (1996). These are given in terms of M_I versus $V-I$ and so are directly comparable with our WFPC2 observations. While the predicted CMDs are similar in terms of their general appearance to the observations (especially model A, which has a constant SFR from 0.02 to 15 Gyr in the past), there are some notable differences that indicate that we cannot simply adopt one of these standard SFH models (such as constant SFR) for the Pegasus dwarf. In this and the following section we model the detailed properties of our observed CMDs to derive the SFH for the Pegasus dwarf.

6.1. *Modeling the Main Sequence*

Normally, upper-MS stars yield an accurate view of the recent SFH, at least in galaxies where such stars are plentiful (see, e.g., Dohm-Palmer et al. 1997b) or obvious MS turnoffs are seen. However, in the Pegasus dwarf the MS is barely populated for $M_V < -2$, and we therefore have a poor statistical base for modeling the recent SFH. What is clear, as it was to earlier investigators, is the relative paucity of stars produced in Pegasus during the past 10^9 years.

In a constant-SFR galaxy, the observed density of MS stars declines rapidly with increasing luminosity because of the combination of the IMF and increasing $t_{\rm MS}$ with decreasing m (see Scalo 1986; Holtzman et al. 1997; Massey 1998). The interpretation of a galactic SFH, therefore, is most straightforward over the time span $t_{\rm MS}[M(\rm min)]$, corresponding to the MS lifetimes of the *least* luminous observable MS stars. However, to find even these older MS stars, we must take an iterative approach and subtract younger stars to reveal less luminous, older MS stars (see Dohm-Palmer et al. 1997b). This is necessary because younger generations will overlie the older, lower mass MS stars. In Pegasus, we reach to $M_V \approx 0$ on the MS, and thus to stars with ages of ≈ 0.5 Gyr.

We used two approaches to fitting the MS, which is well isolated from other evolutionary phases by WFPC2 photometry. From the technique presented by Dohm-Palmer et al. (1997b), we calculated the SFR from the counts in the MS luminosity function. We fitted the observed luminosity function using the stellar evolution models of Bertelli et al. (1994). These provide a mass-magnitude and mass-age relation for the MS at a metallicity of $Z = 0.001$. We use a Salpeter IMF correction and assume the distance modulus to be 24.4. The calculations were performed with the dereddened data, and a completeness correction has been applied. The results shown in Figure 13 are rather noisy, because of the small number of MS stars. The SFR has been approximately constant over the past 100 Myr at ~ 2000 $M_\odot$ Myr^{-1} kpc^{-2}, with a minimum in the SFR occurring between 100 and 200 Myr ago.

We also derived a recent SFH from statistical fits to the CMD using the methods of Tolstoy (1996), as described in §§ 6.2 and 7.4. We adopted simple estimates for the recent SFH and iterated these until satisfactory agreement was achieved between the models and younger components of the CMD. The resulting models for the MS are in Figure 15, which are derived for the SFR given by the solid line in Figure 16. With this technique we attempt to fit all of the younger stars and, thus, do not derive a SFH based solely on the MS. While we can see evidence for fluctuations in the recent SFR over time, we do not find statistically significant SFR variations by more than about a factor of 2.

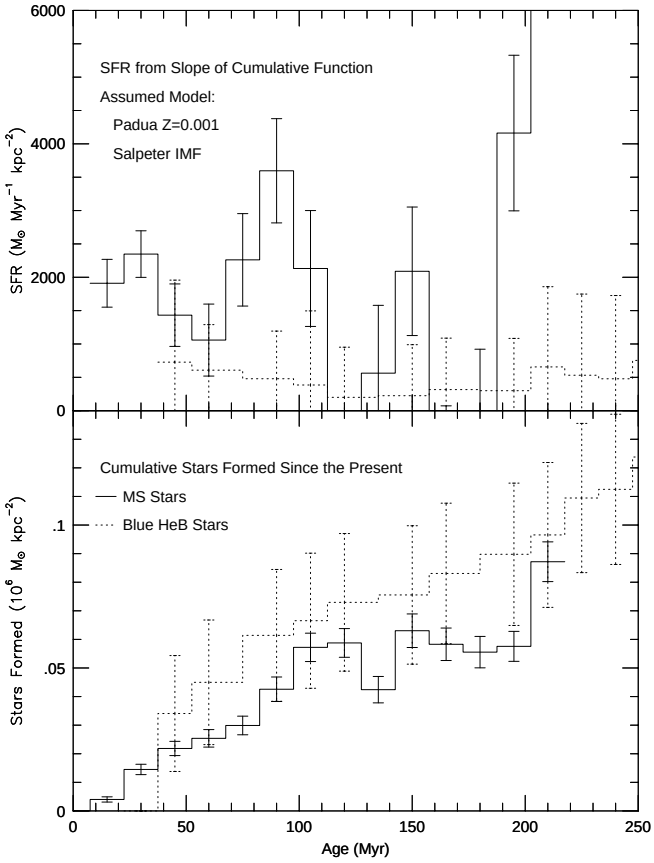

FIG. 13.—*Top*: SFR vs. time derived with the Dohm-Palmer models for the MS and from blue core HeB stars. Error bars refer only to statistical uncertainties. *Bottom*: Cumulative SFRs, which demonstrate the basic agreement between the MS and blue core HeB methods.

Aparicio et al. (1997a) suggest that a factor of 3 spike occurred in the SFR in the Pegasus dwarf about 100 Myr in the past. This would show up in our data as an excess of MS stars near $M_I = -2$; this is the location where the blue MS becomes ill-defined in our data (see Fig. 9, *top*). Our results in Figure 13 agree with those of Aparicio et al., in showing a local peak in the SFR at about 100 Myr, but disagree on the specifics of the evolution out to about 200 Myr, and at all points we must contend with significant amounts of statistical noise. We therefore cannot confirm the Aparicio et al. 100 Myr peak in the SFR from measurements of MS stars in our WFPC2 images.

6.2. *Blue Core Helium Burning Stars*

A second approach to measuring SFH using stars' core HeB evolutionary phases was pioneered by Payne-Gaposchkin (1974), who took advantage of the Cepheid variable pulsation period-age relationship to trace the recent history of star formation in the Large Magellanic Cloud. Our group has also utilized blue core helium

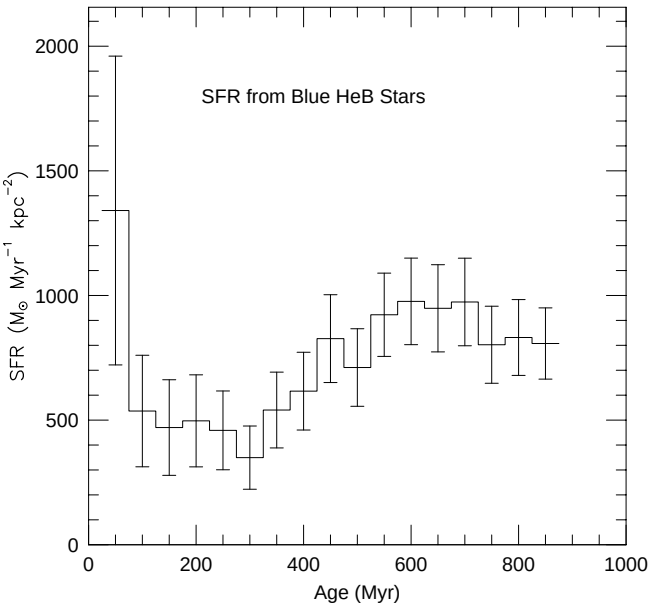

FIG. 14.—SFR as calculated from the luminosity function for stars identified as being in the blue core HeB phase. The bins are 50 Myr wide. The data have been dereddened and corrected for incompleteness. The assumed IMF has a Salpeter slope. The low numbers of candidate blue HeB stars imply a low SFR and contribute fairly large errors to the calculation. For times beyond 800 Myr the photometric errors blend the blue HeB stars and the RC and RGB, making the calculation uncertain.

burning stars to derive SFHs from the numbers of such stars as a function of their luminosity (Dohm-Palmer et al. 1997b).

Stars in their "blue loop" core HeB evolutionary phases are tracers of the recent SFH, because their luminosities scale as a power of the initial mass, and thus luminosity correlates with stellar age. Unfortunately, since the recent SFR in the Pegasus dwarf is very low and the blue core HeB evolutionary phase is short-lived compared with the MS, there is only a scattering of stars in the expected location of blue core HeB stars.

We used two methods to model the observations of blue core HeB stars in the Pegasus dwarf. Tolstoy (1996) presents a statistical approach to deriving a recent SFH from the properties of short-lived stars on a CMD. Since intermediate- and high-mass stars move rapidly in a CMD during their post-MS evolutionary phases, Tolstoy used star number counts in relatively large boxes to statistically compare model predictions with the observations. This approach was applied to our Pegasus CMDs, with fits being made simultaneously to the MS, core HeB, and RGB components of the CMD. We then found that the SFR in Pegasus had increased by about a factor of 2 during the past $\sim$0.5 Gyr (see Fig. 15).

Following Dohm-Palmer et al. (1997b), we also selected candidate blue core HeB stars from our data and generated a luminosity function, from which we calculated the SFR.

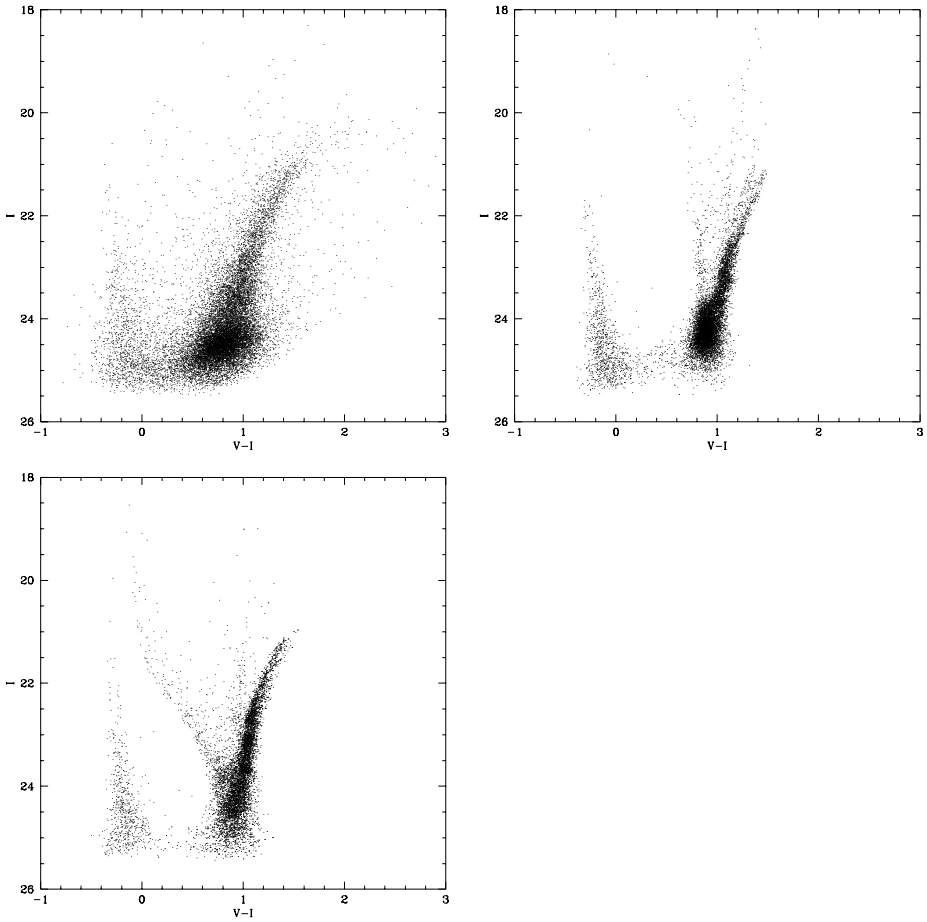

FIG. 15.—Observed CMD for Pegasus (*top left*), compared with two synthetic models computed with the Tolstoy & Saha statistical fitting method. The bottom panel is for our best estimate SFH for $Z = 0.001$ and the top right panel for $Z = 0.004$ based on the Geneva stellar evolutionary tracks. While neither of this pair of models properly fits the blue-loop stars, the lower metallicity is a statistically better option because it includes some stars with intermediate colors that are likely candidates for stars on blue loops.

While this approach of focusing on only one evolutionary phase within a complex stellar population can yield detailed measures of the recent SFH, the low number of blue core HeB stars in Pegasus adds uncertainty to the results. We follow the prescription of Dohm-Palmer et al. (1997b), using the blue HeB mass-magnitude, mass-age, and lifetime relations from Bertelli et al. (1994). Again, we adopt a Salpeter IMF, deredden the data, and apply a completeness correction to the luminosity function.

The results are presented in Figure 14. These are plotted in terms of the SFR per square kiloparsec averaged over the WFPC2 field of view. Error bars reflect only the statistical uncertainties and do not include any corrections for intermediate-color stars that are not in the core HeB phase or are nonmembers of the Pegasus dwarf. The small number of these intermediate-color stars in the WF3 field (see Figs. 3 and 10*a*) indicates that the level of contaminating objects must be low, certainly much less than 50% of the total sample. Therefore, while the SFR derived in Figure 14 is an upper limit, it should not substantially exaggerate the actual SFR.

The approximate agreement between the SFRs found from the MS and blue core HeB stars over the last 100 Myr (2000 and 1350 $M_{\odot}$ Myr^{-1} kpc^{-2}, respectively; see Fig. 13) supports our original assumption that most of the luminous stars in the Pegasus dwarf located between the MS and RGB are on blue loops. This consistency also indicates that rising recent SFRs predicted by our models are likely to be a proper description, and it is also roughly in agreement with the conclusions of Aparicio et al. (1997a).

Because of the low SFR and short lifetime of the blue HeB phase, we have no information from this population for timescales of less than 60 Myr; this is set for the time for intermediate-mass stars to evolve from the MS to the core HeB phase. However, the model in Figure 13 indicates that between 0.1 and 0.4 Gyr ago the SFR was roughly constant at a slightly lower level than the recent SFR. From 0.4 to 0.8 Gyr before the present, the SFR was very close to its current levels. A similar result is derived from the statistical fits to the observed CMDs following the Tolstoy-Saha methodology, as shown by the solid line in Figure 16.

Beyond 800 Myr the photometric errors blend the blue core HeB stars with the RGB, and the star formation history can no longer be determined from the properties of stars that are not associated with the RGB. However, we can still find a range of feasible SFHs by statistically fitting the RGB and also requiring that we produce the correct numbers of extended-AGB and RC stars.

7. LONG-TERM STAR FORMATION HISTORY

7.1. *RGB*

A major division in post-MS evolution occurs for stars with lifetimes of about 1 Gyr and initial masses $\lesssim 2\ M_{\odot}$. These low-mass stars have degenerate helium cores during their RGB evolution and ignite helium burning in a helium flash. This leads to the nearly constant luminosity of the tip of the *old* RGB, which can be a useful distance indicator (see, e.g., Lee et al. 1993a). Following the RGB phase, low-mass stars form an RC or HB during core helium burning and thereafter increase in luminosity along the AGB. More massive stars can evolve on the AGB beyond the RGB tip luminosity and produce an extended AGB before ceasing nuclear burning (see Vassiliadis & Wood 1993).

As a result of this RGB transition between nondegenerate and degenerate ignition of He on the RGB, the luminosity at the tip of the RGB depends upon the mix of stellar ages. During the transition to a low-mass RGB with helium flash at the RGB tip, the luminosity of the tip will increase with *decreasing* stellar mass (see, e.g., Sweigart, Greggio, & Renzini 1990). Thus, for a single-age stellar population the location of the RGB tip is predicted to move toward higher luminosity and redder colors as a simple stellar population ages between about 0.5 and 1.2 Gyr. Therefore, any galaxy that experienced extensive amounts of star formation during the past ≈ 1 Gyr may have a complex RGB tip.

The RGB in Pegasus displays a moderate range in color; the change in $V-I$ color between the location of the RC and its roughly defined tip is only 0.5–0.6 mag. Such steeply rising RGBs are characteristic of either moderately metal-poor old stars (see, e.g., Lee et al. 1993a; their calibration suggests [Fe/H] ≈ -1.5) or of relatively massive young stars, whose RGB tracks at a given metallicity are bluer at than those of low-mass stars. That Pegasus cannot contain a pure, old RGB can be seen from the presence of intermediate-mass MS stars, the intermediate-age RC, and the lack of a sharply defined RGB tip; old RGB stars may be present in the Pegasus dwarf, but will be challenging to cleanly detect.

The difficulty in distinguishing older RGB stars in a CMD can be illustrated by considering ages of stars on the upper part of the RGB for a simple constant-SFR model. Stellar evolution models show that the RGB lifetime at luminosities above the RC are almost independent of initial mass for $M \leq 1.5\ M_{\odot}$, or for stellar nuclear burning lifetimes to the RGB tip of more than 1.5 Gyr. In this case, the number of stars on the upper RGB is approximately given by

$$\psi_0(t_{\rm gal} - 1.5\ {\rm Gyr}) \int_{M_{\rm RT}({\rm min})}^{M_{\rm RT}({\rm max})} \phi(m) dm\ ,$$

where $M_{\rm RT}$(min) is defined as the initial mass of stars with lifetimes at the RGB tip of the age of the galaxy, $t_{\rm gal}$, and $M_{\rm RT}$(max) $\approx 2\ M_{\odot}$ is the mass of the most massive stars to reach the RGB tip. Therefore, the number of upper RGB stars approaches being proportional to the age of the galaxy in long-lived systems, and stars born, for example, in the first 4 Gyr of a 14 Gyr–old, constant-SFR galaxy will make up about 25% of this number. Unless these oldest stars have an obvious signature that cannot be produced by a younger stellar population component, such as an associated blue HB, they are not readily identified as unique contributors to an observed CMD.

The detectability of the oldest stars also depends on the SFH and the age-metallicity relationship. If the SFR was higher when a galaxy was young, then there are more old stars, and detection is more likely. Conversely, galaxies that had increasing SFRs during their youths can be difficult places in which to find older stars. For this reason we have not chosen to consider more complicated SFH models in which age and metallicity both vary. While such models can be constructed (e.g., Aparicio et al. 1997a) and are required in some cases (e.g., Einsel et al. 1995; Han, Hoessel, & Gallagher 1998), they are not justified in the Pegasus dwarf, where we have yet to find any discernible signs of an age-metallicity relationship. If we were to adopt an age-metallicity correlation, then this ad hoc assumption would almost entirely determine our derived SFH for the

intermediate-age and old stellar populations. Measurements of the stellar age-metallicity relationship are required to overcome this important ambiguity.

7.2. *Red Clump and Related Issues*

Our WFPC2 data show an excess density of stars on the *VI* CMD overlying the RGB near $I = 24.5$ (see Fig. 6). These stars are in core helium burning evolutionary phases. The distribution of red helium-burning stars depends sensitively on initial mass, amount of mass loss, and metallicity, but such stars may be classified into three main categories: intermediate-mass stars at the base of the blue loop, RC stars that have experienced a helium flash at the tip of the RGB, and old, red HB stars. The latter possibility seems unlikely, since the mean color of the RC region is not offset to bluer colors, as is expected for a true red horizontal branch (cf. the HB seen in NGC 147 data, shown in Fig. 9). Further consideration is given to the possibility that most of these stars either are associated with the RC or are more massive stars that did not experience helium ignition in a degenerate core.

Each of these models implies a different SFH for the Pegasus dwarf. One model produces most of the RC helium-burning stars by invoking an epoch of enhanced star formation about 1 Gyr ago (Fig. 16, *dashed line*). Stars made at this time have very short red giant lifetimes and relatively long core helium burning lifetimes in the red. This model thus yields a high density of red stars at the required luminosity. It also implies that a strong MS turnoff associated with a relatively high-amplitude burst should exist at about 1 mag fainter than our data, as well as a well-populated extended AGB. This model requires considerable fine-tuning, as the transition between the RC and blue loop occurs over a very small range of mass and is very sensitive to metallicity, while we do not see many blue loop stars, which should be plentiful in what is essentially a postburst galaxy.

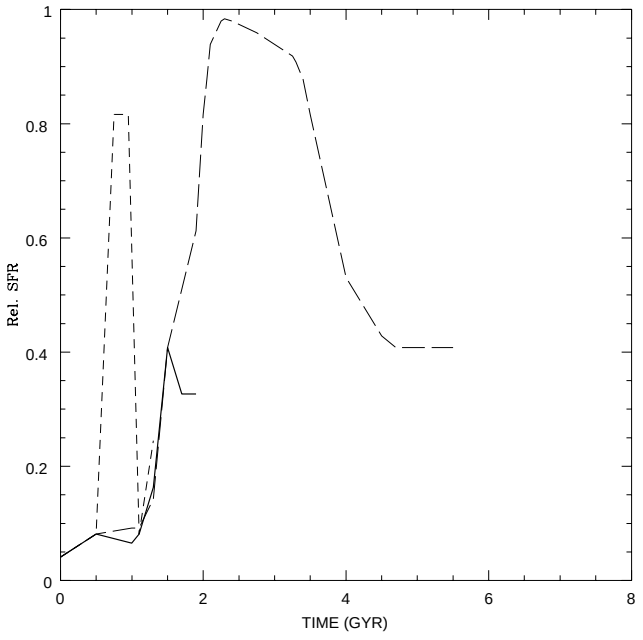

FIG. 16.—SFH models derived from statistical fits to our WFPC2 photometry of the Pegasus dwarf, shown in terms of *relative* SFRs. The solid line is the recent SFH based on the MS, blue-loop stars, and the blue side of the RGB with $Z = 0.001$. This is the best constrained component of the model. The short-dashed line shows a high-metallicity ($Z = 0.004$) model in which most stars are less than 1 Gyr old. This model fits the shape of the CMD, but produces no stars as blue as the observed blue-loop candidates and has difficulty explaining the AGB population. The long-dashed line is a speculative SFH model designed to match the RGB. Since we assume constant metallicity, the width in color of the RGB depends only on the range of stellar ages. If metallicity declines with increasing age, then the height of the peak declines and its width increases, i.e., the mean SFR drops and the galaxy becomes older.

The second and preferred interpretation assumes that the observed excess of stars superposed on the lower RGB are a classical post-RGB RC. In this case, the RC phase lifetimes are about 85–70 Myr for initial mass 0.9–2 $M_\odot$ stars with $Z = 0.001$ (see, e.g., Seidel, Demarque, & Weinberg 1987). The lifetime on the RGB for stars at luminosities equal to or higher than the RC are constant at about 50 Myr for stars with initial masses of about 1.5 $M_\odot$ or less, and decrease as the upper mass bound for stars that undergo helium flashes at the RGB tip is reached (see, e.g., Sweigart et al. 1990). For example, in the Geneva models with $Z = 0.001$ the RGB lifetime for $\log L \geq 1.8$ is 52–53 Myr for 0.9–1.5 $M_\odot$ stars, dropping to 31 Myr for an initial mass of 1.7 $M_\odot$. Thus, a high ratio of RC to RGB stars would be a strong signature of enhanced star formation within the past 2 Gyr or more.

Our WFPC2 photometry of stars in the Pegasus dwarf does not yield a straightforward determination of the ratio $N(\mathrm{RGB})/N(\mathrm{RC})$, because the observational errors (and thus also incompleteness) are a significant factor at the luminosity of the RC. However, using models of the upper RGB, which include corrections for incompleteness, to estimate how many RGB stars are superposed on the RC region, we estimate $N(\mathrm{RGB}) \approx 6000$ stars and $N(\mathrm{RC}) \approx 9500$ stars, or $N(\mathrm{RGB})/N(\mathrm{RC}) \approx 0.6$. The lifetimes of these two evolutionary phases for stars with ages of over 2 Gyr predict a ratio of 0.60. This agreement implies that *most* of the stars that we now see in the RGB and RC of the Pegasus dwarf were formed more than ≈ 2 Gyr ago.

7.3. *Extended Asymptotic Giant Branch*

The Pegasus dwarf resembles other nearby irregular galaxies, including the Magellanic Clouds (see, e.g., Mould & Reid 1987), in having a well-defined extended AGB (Aparicio & Gallart 1995). Stars on the extended AGB are more luminous than the RGB tip and often have lower effective temperatures and, therefore, redder colors than the RGB tip region. M. Aaronson and collaborators (e.g., Cook, Aaronson, & Norris 1986) were among the first to demonstrate that luminous AGB stars are useful indicators of the presence of intermediate-age stars in galaxies beyond the Milky Way's family.

More recently, Gallart et al. (1994, 1996) incorporated extended-AGB stars in their investigation of the SFH of the Local Group IBm galaxy NGC 6822. They emphasized the connection between the detection of bright AGB stars and existence of a stellar population with ages between 1 and 10 Gyr, but they also noted some of the uncertainties involved with the interpretation of these types of stars. In particular, the extended AGB is sensitive to stellar metallicities and mass-loss rates, neither of which can be reliably determined from *BVI* CMDs of a mixed-age stellar population where the SFH is unknown. In Pegasus there are about 100 stars on the extended AGB, yielding a ratio to the number of RC stars of about 10^{-3}. This is consistent with the theoretical predictions for lifetimes of extended AGB stars produced by intermediate-age stellar populations, which are only $\approx 0.1\%$ of the helium-burning lifetime.

Unfortunately, the true situation regarding the properties of the extended AGB may be even more complicated. Guarnieri, Renzini, & Ortolani (1997) reviewed a variety of additional factors that may influence the populations of AGB stars in galaxies, including the importance of binary systems. Also, dust in the winds of luminous AGB stars affects their optical magnitudes and colors; the CMD of luminous extended-AGB stars is therefore difficult to quantitatively interpret.

7.4. *Summary of the Long-Term Evolution*

Pegasus contains a pronounced RGB with a well-populated RC. The tip of the RGB is diffuse, as is typical in intermediate-age stellar systems. The ratios $N(\mathrm{RC})/N(\mathrm{RGB})$ and $N(\mathrm{extended-AGB})/N(\mathrm{RC})$ are consistent with predictions for stellar populations that formed their stars 2–6 Gyr before the present. We conclude that in Pegasus the structure of the "red plume" tells us that the bulk of stars now on the RGB formed more than 1–2 Gyr ago. In addition, the extended AGB is too sparsely populated to agree with models in which most of the star formation occurred more recently than 1–2 Gyr before the present. While an older, very metal-poor stellar population cannot be excluded, it should comprise a minority of the RGB stars seen in our CMD for the Pegasus dwarf.

Constant-metallicity models are illustrated in Figure 15. These produce a relatively young age for the bulk of the stars, most of which form in these models from 2 to 4 Gyr ago, when the average SFR was about 10 times its current value. Incorporating declining metallicity levels in older stars may be a more realistic assumption. In this class of model, the structure of the RGB depends on both age and metallicity. A general feature of such models will be a more prolonged epoch of star formation. In our best estimate for this type of model, the primary star-forming epoch would extend back to about 8 Gyr ago. The average SFR, then, is reduced by about a factor of 3 relative to the constant stellar metallicity model. This reflects the longer time span of active star formation, and that older stars on the RGB are more numerous on account of the form of the IMF.

A purely bimodal model for the stellar age distributions, in which a trace ≤ 1 Gyr age stellar component is seen in combination with a very old, low-metallicity stellar population, is excluded. This SFH predicts a narrow, relatively blue RGB with a sharply defined RGB tip, which we do not see. A bimodal SFH model also fails to produce the observed populous RC that is approximately centered on top of the RGB.

7.5. *Pegasus at Its Peak*

Our "young" model, in which most of the stars in Pegasus are produced during about 2 Gyr, reaches its maximum luminosity at the end of the main star-forming epoch, about 2 Gyr before the present. Estimating a current stellar mass for the Pegasus dwarf of $(1\text{–}2) \times 10^7\ M_\odot$ from its integrated colors and optical luminosity (see Table 1), we can then calculate the peak luminosity. Stellar population evolution models, such as those of Möller, Fritze–von Alvensleben, & Fricke (1997), predict that after 2 Gyr, with a constant SFR, $M/L_V \approx 1$. At maximum light our rapid astration model for Pegasus would have had $M_V \approx -14$. The color depends on the metallicity distribution of the stars, but would fall in the range $0.1 \leq B-V \leq 0.3$. Even at its best, Pegasus might not have been a notable galaxy.

The SFH models that we have obtained for Pegasus allow the primary star-forming phase to extend up to 8 Gyr. In this case, the galaxy would be about 1 mag fainter 2 Gyr ago, and its color would be considerably redder, e.g., $B-V \approx 0.4$. The only way for the Pegasus dwarf to have been more luminous than a dwarf is for it to have experienced a major starburst where a significant fraction of the total stellar mass forms in ≈ 0.1 Gyr (Babul & Ferguson 1996). We have yet to find any compelling direct evidence for such an event (e.g., remnant populous star clusters or well-defined MS turnoffs), but we also cannot exclude the possibility of a major starburst, especially if it occurred more than 2 Gyr ago. However, the simplest model for the SFH of the Pegasus dwarf galaxy assumes that stars formed at relatively constant rate over several Gyr, with the main episode of star formation ending about 2 Gyr before the present.

7.6. *Comparisons with Dwarf Spheroidal Galaxies*

The larger of the Local Group dSph systems are similar to Pegasus in terms of size and luminosity. The Galactic dSph's are well known to contain examples of purely old, metal-poor galaxies, such as the Draco, Sculptor, and Ursa Minor galaxies (see review by Gallagher & Wyse 1994). However, more recently evidence has been growing for recent star formation in dSph's, including the galaxies Carina (Smecker-Hane et al. 1994) and Leo I (Lee et al. 1993b; Demers, Irwin, & Gambu 1994; see also Da Costa 1998). These results prove that some Galactic companion dSph's have undergone episodic star formation, the impact of which on the metallicities of the stellar populations is unclear. The effects of the star formation episodes are directly seen in the multiple MS turnoffs in Carina, but also leave their mark in the form of composite HB/RC structures in the observed CMDs.

Additional examples of complicated SFH in very small galaxies can be found in dSph and related objects elsewhere in the Local Group. These galaxies also show a range in SFHs. Andromeda I (van den Bergh 1972, 1974) likely has an intermediate to old stellar population, and Da Costa et al. (1996) estimate a mean stellar age of about 10 Gyr from their WFPC2 photometry. On the other hand, the transition Local Group dwarf LGS 3 contains H I gas and probably some intermediate-age (<1 Gyr) stars, as well as more extensive old populations (Aparicio, Gallart, & Bertelli 1997b; Mould 1997; Young & Lo 1997). Evidently whatever physical "clock" sets the timescale for star formation in these small galaxies is quite variable and does not simply depend on galaxy size or its eventual location within the Local Group (see, e.g., Gallagher & Wyse 1994; Da Costa 1998).

8. DISCUSSION AND CONCLUSIONS

The Pegasus dwarf irregular galaxy is a nearby, low-SFR, low-mass dwarf galaxy. Our revised distance to the Pegasus dwarf of 760 kpc places this galaxy in the M31 "family," but at a projected distance on the sky of 400 kpc, it is unlikely to be bound to M31. Pegasus is probably a small, independent member of the Local Group.

The established interstellar gas reserves in Pegasus from the measured H I content suggest that the ratio of gas (including cosmic He) to stellar mass is $M_g/M_* = 0.2$. Pegasus lacks the raw material to substantially enlarge its stellar mass but is not yet a stellar fossil. At the present time

its SFR is low, $SFR_0 \approx 3 \times 10^{-4}\ M_\odot\ yr^{-1}$, and the timescale to exhaust the gas at this rate is 13 Gyr. The lifetime average SFR is several times higher, so it is possible that a return to normal SFRs could result in gas exhaustion within a few gigayears. Pegasus is like many other irregular galaxies where star formation is "down but not out" (see Hunter 1997).

Our observed CMDs for the Pegasus dwarf obtained with WFPC2 in the equivalent of *BVI* colors show a sparsely populated MS and a complicated "red plume" consisting of a fairly broad RGB, a pronounced RC (cleanly detected here for the first time), and an extended AGB. The extended AGB covers much of the optical galaxy on ground-based images taken with the WIYN telescope. Our quantitative analysis of these CMDs establishes the following: (1) The reddening of $E(B-V) = 0.15$ is higher than previously thought. This mainly accounts for our reduction in distance from $D = 960$ kpc found by Aparicio (1994) to $D = 760 \pm 100$ kpc. (2) Star formation is ongoing at a low level and has produced at least one H II region, a blue MS, and core HeB blue loop stars. (3) The RGB is prominent, densely populated, and relatively blue. (4) The presence of a pronounced RC, the width of the RGB, and the lack of a well-defined tip of the RGB are all indicators of a strong intermediate-age stellar population component.

We have quantitatively modeled the SFH for Pegasus by fitting our observed CMDs following the methodologies of Tolstoy & Saha (1996) and Dohm-Palmer et al. (1997b). The short-term trend in SFR shows a modest decline in SFR during the past 0.5 Gyr from the densities of MS and blue core HeB stars as functions of luminosity. The Pegasus dwarf therefore shows a slowly varying recent mean SFR, but nothing that would qualify as a recent starburst.

Our data are not sufficiently deep to yield a unique description of the SFH over more than ≈ 1 Gyr. Instead, we find a spectrum of possible models for the long-term SFH of the Pegasus dwarf. At one extreme is a rapid evolution model that makes most of the stars between 2 and 4 Gyr before the present and assumes constant metallicity at $Z = 0.001$. At the other extreme are less well defined models, where metallicity declines in older stars; these models have lower SFRs spread over longer time intervals, extending perhaps to 10 Gyr in the past.

The historical optical characteristics of Pegasus depend on its SFH. However, for models where the SFR has been roughly constant at intermediate ages of a few gigayears, it would have been most luminous ($M_V \approx -14$) and relatively blue when its SFR began its recent decline about 2 Gyr ago. Even at its peak, Pegasus was most likely a "dwarf" in terms of absolute magnitude.

A galaxy like Pegasus in our most actively star-forming model would be brightest at a look-back time of ≈ 2 Gyr, or a redshift of $z \approx 0.2$. At this distance, a Pegasus-like actively star-forming dwarf would have $V \sim 26$, blue colors, and an angular size of less than 0.″5. Thus, this type of object could resemble some of the low-redshift, faint blue galaxies (see, e.g., Odewahn et al. 1996).

If the Pegasus dwarf were to lose its gas supply, it might structurally resemble a spheroidal dwarf galaxy. Lo et al. (1993) showed the H I velocity field in Pegasus to be fairly chaotic. They place an upper limit of 5 km s^{-1} on gas rotation and measure a local velocity dispersion of about 5 km s^{-1} and a global dispersion of 9 km s^{-1}. Interestingly, stars formed from gas with these random velocities would likely retain a velocity dispersion similar to that found in the most luminous of the Galactic dSph galaxies (e.g., Gallagher & Wyse 1994). Furthermore, the global rotation is sufficiently slow that the ratio of the stellar velocity dispersion to rotational velocity also is likely to be greater than 1, and so the older stellar body of the Pegasus dwarf probably has a spheroidal rather than thin disk structure and resembles a low-luminosity dE or dwarf spheroidal galaxy. Measurements of stellar kinematics would test this possibility, and could be made through observations of the relatively bright extended-AGB stars in the Pegasus dwarf.

Stellar photometry at the level of the HB will similarly enhance our ability to constrain the long-term SFH of the Pegasus dwarf. The blue HB that is seen in And I (Da Costa et al. 1996) and NGC 147 (Han et al. 1997) demonstrates the existence of old, metal-poor stellar populations while also yielding reliable distances. Evidently these two spheroidal galaxies made most of their stars over a time span of several gigayears centered at about 8–10 Gyr before the present. In comparing the Pegasus dwarf with these galaxies we need to establish the importance of its very old (>8 Gyr), metal-poor stellar population component, which defines the level of star-forming activity during the primary epoch of giant galaxy formation. By way of contrast, in the LMC such stars are rare (Olszewski, Suntzeff, & Mateo 1996), and we would like to know whether this is a general distinction between the irregular and spheroidal dwarf galaxies. This information is essential in charting possible relationships between present-epoch dwarf galaxies and faint blue galaxies seen at moderate to high redshifts corresponding to look-back times exceeding several gigayears.

The improvements in the quantitative analysis of stellar populations in nearby galaxies made possible by WFPC2 on *HST* prove that despite its small mass, the Pegasus dwarf has had an extended evolutionary history; this galaxy has likely supported star formation for at least 3 Gyr. The attractive idea that very small galaxies should experience a single primary and possibly cataclysmic episode of star formation during their lifetimes does not appear to hold for the Pegasus dwarf or many other low-mass Local Group galaxies. We are then left with the intriguing problems of understanding what physical mechanisms allow some small galaxies to produce their stars slowly and without violence, and how this relates to the variety of stellar age mixes and gas contents found in extreme dwarf galaxies in the nearby universe.

Support for this work was provided by NASA through grant GO-5915 from the Space Telescope Science Institute, which is operated by the Association of Universities for Research in Astronomy, Inc., under NASA contract NAS 5-26555. This research has made use of the NASA/IPAC Extragalactic Database (NED), which is operated by the Jet Propulsion Laboratory, California Institute of Technology, under contract with NASA. E. T. thanks Ralph Bohlin for research support during the early phases of this project. J. S. G. expresses his appreciation for partial travel support from Space Telescope European Coordinating Facility, which made visits to Garching possible. We thank an anonymous referee for comments that improved this paper.

REFERENCES

Aparicio, A. 1994, ApJ, 437, L27
Aparico, A., & Gallart, C. 1995, AJ, 110, 2105
Aparicio, A., Gallart, C., & Bertelli, G. 1997a, AJ, 114, 669
———. 1997b, AJ, 114, 680
Aparicio, A., Gallart, C., Chiosi, C., & Bertelli, G. 1996, ApJ, 469, L97 (erratum 479, L153 [1997])
Babul, A., & Ferguson, H. C. 1996, ApJ, 458, 100
Bertelli, G., Bressan, A., Chiosi, C., Fagotto, F., & Nasi, E. 1994, A&AS, 106, 275
Burstein, D., & Heiles, C. 1984, ApJS, 54, 33
Charbonnel, C., Meynet, G., Maeder, A., Schaller, G., & Schaerer, D. 1993, A&AS, 101, 415
Christian, C. A., & Tully, R. B. 1983, AJ, 88, 934
Cook, K. H., Aaronson, M., & Norris, J. 1986, ApJ, 305, 634
Da Costa, G. S. 1998, in Stellar Astrophysics for the Local Group, ed. A. Aparicio & A. Herrero (New York: Cambridge Univ. Press), in press
Da Costa, G. S., Armandroff, T. E., Caldwell, N., & Seitzer, P. 1996, AJ, 112, 2576
Dekel, A., & Silk, J. 1986, ApJ, 303, 39
Demers, S., Irwin, M. J., & Gambu, I. 1994, MNRAS, 266, 7
Diplas, A., & Savage, B. D. 1994, ApJ, 427, 274
Dohm-Palmer, R. C., et al. 1997a, AJ, 114, 2514
———. 1997b, AJ, 114, 2527 (addendum 115, 152 [1998])
Einsel, C., Fritze–von Alvensleben, U., Krüger, H., & Fricke, K. J. 1995, A&A, 296, 347
Fagotto, F., Bressan, A., Bertelli, G., & Chiosi, C. 1994, A&AS, 105, 29
Ferrara, A., & Tolstoy, E. 1998, in preparation
Fisher, J. R., & Tully, R. B. 1975, A&A, 44, 151
Fitzpatrick, E. L. 1985, ApJ, 299, 219
Fruchter, A., & Hook, R. 1997, in The *Hubble Space Telescope* and the High Redshift Universe, ed. N. R. Tanvir, A. Aragon-Salamanca, & J. V. Wall (Singapore: World Sci.), 137
Gallagher, J. S., et al. 1996, ApJ, 466, 732
Gallagher, J. S., & Wyse, R. F. G. 1994, PASP, 106, 1225
Gallart, C., Aparicio, A., Bertelli, G., & Chiosi, C. 1996, AJ, 112, 1950
Gallart, C., Aparicio, A., Chiosi, C., Bertelli, G., & Vílchez, J. M. 1994, ApJ, 425, L9
Goodwin, S. P. 1997, MNRAS, 286, 669
Guarnieri, M. D., Renzini, A., & Ortolani, S. 1997, ApJ, 477, L21
Han, M., Hoessel, J. G., & Gallagher, J. S. 1998, in preparation
Han, M., et al. 1997, AJ, 113, 1001
Hensler, G., Gallagher, J. S., & Theis, C. 1998, in preparation
Hodge, P. 1980, ApJ, 241, 125
Hoessel, J. G., Abbott, M. J., Saha, A., Mossman, A. E., & Danielson, G. E. 1993, AJ, 100, 1151
Hoessel, J. G., & Mould, J. R. 1982, ApJ, 254, 38
Hoffman, L., Salpeter, E. E., Farhat, B., Roos, T., Williams, H., & Helou, G. 1996, ApJS, 105, 269
Holmberg, E. 1958, Medd. Lunds Astron. Obs., Ser. II, No. 128
Holtzman, J. A., Burrows, C. J., Casertano, S., Hester, J. J., Trauger, J. T., Watson, A. M., & Worthy, G. 1995, PASP, 107, 1065
Holtzman, J. A., et al. 1997, AJ, 113, 656
Hunter, D. 1997, PASP, 110, 937
Hunter, D. A., Hawley, W. M., & Gallagher, J. S. 1993, AJ, 106, 1797
Ivanov, G. R. 1996, A&A, 305, 708
Karachentsev, I. 1996, A&A, 305, 33
Karachentseva, V. E., Karachentsev, I. D., Richter, G. M., von Berlepsch, R., & Fritze, K. 1987, Astron. Nachr., 308, 247
Lattanzio, J. C. 1991, ApJS, 76, 215
Laureijs, R. J., Helou, G., & Clark, O. F. 1994, in ASP Conf. Ser. 58, The First Symposium on the Infrared Cirrus and Diffuse Interstellar Clouds, ed. R. M. Cutri & W. B. Latter (San Francisco: ASP), 133
Lee, M. G., Freedman, W. L., & Madore, B. F. 1993a, ApJ, 417, 553
Lee, M. G., Freedman, W., Mateo, M., Thompson, I., Roth, M., & Ruiz, M.-T. 1993b, AJ, 106, 1420
Leitherer, C. 1995, in *HST* Data Handbook (Baltimore: STScI), 520
Lo, K.-Y., Sargent, W. L. W., & Young, K. 1993, AJ, 106, 507
Marlowe, A. T., Heckman, T. M., Wyse, R. F. G., & Schommer, R. 1995, ApJ, 438, 563
Massey, P. 1998, in ASP Conf. Ser. 142, The Stellar Initial Mass Function, ed. D. J. Howell, G. F. Gilmore, & I. R. Parry (San Francisco: ASP), in press
Meurer, G. R., Freeman, K. C., Dopita, M. A., & Cacciari, C. 1992, AJ, 103, 60
Miller, B. W. 1996, AJ, 112, 991
Möller, C. S., Fritze–von Alvensleben, U., & Fricke, K. J. 1997, A&A, 317, 676
Mori, M., Yoshii, Y., Tsujimoto, T., & Nomoto, K. 1997, ApJ, 478, L21
Mould, J. 1997, PASP, 109, 125
Mould, J., & Reid, N. 1987, ApJ, 321, 156
O'Connell, R. W., Gallagher, J. S., & Hunter, D. A. 1994, ApJ, 433, 650
Odewahn, S. C., Windhorst, R. A., Driver, S. P., & Keel, W. C. 1996, ApJ, 427, L130
Olszewski, E. W., Suntzeff, N. B., & Mateo, M. 1996, ARAA, 34, 511
Payne-Gaposchkin, C. 1974, Smithsonian Contrib. Astrophys., No. 16
Rozanski, R., & Rowan-Robinson, M. 1994, MNRAS, 271, 530
Saha, A., Sandage, A., Labhardt, L., Tammann, G. A., Macchetto, F. D., & Panagia, N. 1996, ApJ, 466, 65
Sandage, A. 1986, AJ, 91, 496
Sandage, A., & Fomalant, E. 1993, ApJ, 407, 14
Scalo, J. 1986, Fundam. Cosmic Phys., 11, 1
Schaller, G., Schaerer, D., Meynet, G., & Maeder, A. 1992, A&AS, 96, 269
Schechter, P., Mateo, M., & Saha, A. 1993, PASP, 105, 1342
Seidel, E., Demarque, P., & Weinberg, D. 1987, ApJS, 63, 917
Skillman, E. D., Bomans, D. J., & Kobulnicky, H. A. 1997, ApJ, 474, 205
Smecker-Hane, T. A., Stetson, P. B., Hesser, J. E., & Lehnert, M. D. 1994, AJ, 108, 507
Sweigart, A. V., Greggio, L., & Renzini, A. 1990, ApJ, 364, 527
Tolstoy, E. 1996, ApJ, 462, 684
Tolstoy, E., & Saha, A. 1996, ApJ, 462, 672
Tolstoy, E., et al. 1998, in preparation
Tosi, M., Greggio, L., Marconi, G., & Focardi, P. 1991, AJ, 102, 951
van den Bergh, S. 1972, ApJ, 171, L31
———. 1974, ApJ, 191, 271
Vassiliadis, E., & Wood, P. R. 1993, ApJ, 413, 641
Young, L. M., & Lo, K.-Y. 1997, ApJ, 490, 710